Mode Crystallography of distorted structures

J. M. Perez-Mato, D. Orobengoa and M. Aroyo

Departamento de Fisica de la Materia Condensada, Facultad de Ciencia y Tecnologia,
Universidad del Pais Vasco (UPV-EHU), Apdo. 644, 48080 Bilbao, Spain

1. Introduction

Many crystalline structures can be considered pseudosymmetric with respect to some configuration of higher symmetry. This higher symmetry arrangement may be another phase of the compound or can be a virtual reference structure. In the following we will call this structure (real or virtual) of higher symmetry, *parent* structure or *parent* phase. The actual structure can then be qualified as a *distorted* structure and may be described as a parent crystalline structure plus a static symmetry-breaking structural distortion [REF1]. A group-subgroup relation necessarily exists between the space groups of the parent structure and the distorted one. If the distortion is sufficiently small, a thermally driven structural transition to the configuration of higher symmetry may take place at higher temperatures [REF2]. Ferroic structures are a particular case of this type of distorted structures, with the distorted (ferroic) structure having a lower point group than the parent phase [REF3]. Structural distortions can be of displacive type or may include some type order-disorder component (symmetry breaking change of the occupation probabilities of some atomic sites). In the present paper, we will only consider purely displacive distorted structures, and the term *distorted* will be used in this restricted sense. We will see below however that some simple order-disorder distortions can also be included in this displacive formalism.

Similarly as it happens with dynamic distortions (thermal vibrations), we know since the development of Landau theory [REF4] that the natural language to deal with the static frozen distortions present in ferroic structures and distorted structures in general, is the one of *modes*. Modes are collective correlated atomic displacements fulfilling certain symmetry properties. Structural distortions in distorted structures can be decomposed into contributions from different modes with symmetries given by irreducible representations of the parent space group. One can then distinguish primary and secondary (induced) distortions with different symmetries, which will have in general quite different weights in the structure, and will respond differently to external perturbations. In general, the use of symmetry-adapted modes in the description of distorted structures introduces a natural physical hierarchy among the structural parameters. This can be useful not only for investigating the physical mechanisms that stabilize these phases, but also for pure crystallographic purposes. The set of structural parameters used in a mode description of a distorted phase will in general be better adapted for a controlled refinement of the structure, or for instance for comparative

studies between different materials.

Despite its obvious advantages the use of symmetry adapted modes is still scarce in crystallographic studies of distorted structures. Examples regularly appear in the literature where this approach is applied in a quantitative and systematic form [REF5], in the sense of characterizing the different symmetry components present in the structure, but the approach still is minoritary. During many years there has been one clear reason for that situation, namely, the mode decomposition analysis in non-trivial cases required a deep knowledge of group theory and considerable calculation effort for each specific case. In the last years, this situation has changed. Free computer programs have been developed which allow fast and automatic mode analyses [REF6]. These tools have focussed on the calculation of the basis of distortion modes relevant in each case. However, this has been usually done within the setting of the parent structure, without using the space group symmetry of the distorted structure in an explicit form. This has implied in general a formalism and parameterization quite distant from the usual crystallographic description, and probably has hampered its systematic use among crystallographers.

To improve this situation we have recently made available in the Bilbao crystallographic server [REF7] a tool (AMPLIMODES) that allows the automatic mode decomposition of any pseudosymmetric structure [REF8]. The program provides, apart from a basis of symmetry modes, also their amplitudes in the given structure. An important feature of the program is that the paramerization of the structural distortion is done in a form close to the conventions of crystallography. Modes are given in terms of relative displacements for the asymmetric unit of the distorted phase, so that the actual atomic positions describing the structure in the conventional approach are readily obtained from the listed modes and their amplitudes. By this means we pretend to introduce a parameterization that facilitates the switch from the symmetry mode approach to the conventional description of a structure, and hopefully will help to standardize and generalize its use in crystallographic studies.

A further step in this direction has been the adaptation of the refinement program FullProf [REF9] and of AMPLIMODES for their combined use, so that now FullProf can use directly the output of AMPLIMODES and refine distorted structures using as refinable parameters the amplitudes of the basis of symmetry modes provided by this

latter. The potential of the symmetry-mode approach for the determination of pseudosymmetric or distorted structures, with the introduction among the structural parameters of a strong hierarchy and the reduction of correlations, has recently been demonstrated [REF10-Campbell] for a specific case. We hope that this automatic combination of the two programs will ease the application of the direct symmetry-mode refinement of distorted structures and will extend its use, advancing in the development of a standardized "Mode Crystallography".

Within this context, we present in this article a series of illustrative examples of the virtues and possibilities of the analysis of distorted structures in terms of symmetry-adapted modes. All the results presented here have been obtained using the above mentioned program, AMPLIMODES. In a subsequent article we will show also with some examples the direct application of this approach to the refinement problem using Fullprof [REF9].

2. Symmetry-Mode description of distorted structures

We review in this section the basic features of the symmetry-adapted mode description of distorted structures. By this means we introduce the notation and parameterization employed. In order to simplify the notation, we will avoid when possible any explicit indication of the parameters describing the symmetry properties of the modes (wave vectors, wave vector stars, etc…). Thus, we reduce the notation to the basic features which are really needed in a practical case, assuming that we have some computing tool to obtain a basis of symmetry-adapted modes, given in the crystallographic format explained below, as is done by AMPLIMODES.

The distortion relating a parent structure with the actual displacively distorted structure of lower symmetry can be deconvoluted into two parts:

i) A set of atomic displacements which may break some translational symmetry but keep the metrics of the underlying lattice, so that the basis vectors of the resulting new Bravais lattice are exactly given by some integer combination of the primitive unit cell basis vectors of the parent structure.

ii) A strain of the lattice mentioned in i)

This separation corresponds to the distinction of the elastic degrees of freedom from the internal atomic degrees of freedom in the structure, and is done automatically if the atomic displacements and positions are expressed in relative coordinates with respect to the cell parameters, as usually done in crystallography.

In general, for full consistency and formal rigor (orthogonal properties of modes, etc…), the mode analysis should be done assuming that the relative coordinates of the distorted structure correspond to step i) above, i.e. to a structure with an unstrained lattice, so that its unit cell perfectly matches that of the parent structure. The additional strain present in the real structure can be added automatically *a posteriori*, by taking the *real* unit cell, keeping the same relative coordinates.

Let $r_o(\mu)$ be the positions of the atoms μ (μ=1,…s) within an asymmetric unit of the parent structure with space group G. The asymmetric unit of the observed distorted structure with lower space group H, subgroup of G, will in general have a larger number of atoms due to the splitting of the Wyckoff orbits of the higher-symmetry space group [REF12]. Its atomic positions can then in general be expressed as

$$\mathbf{r}(\mu,i) = \mathbf{r}_o(\mu,i) + \mathbf{u}(\mu,i) \qquad (1)$$

where $\mathbf{r}_o(\mu,i)$ (μ=1,…,s; i=1,…,n_μ) are the atomic positions of the parent structure, expressed in the setting of the low symmetry space group, with the index i enumerating the formally splitted atomic orbits coming from a single Wyckoff orbit in G.

The set of atomic displacements u(μ,i) within an asymmetric unit of the distorted structure fully defines the displacive distortion relating both structures. In general, it can then be expressed as the sum of the contributions of a basis of symmetry-adapted modes:

$$\mathbf{u}(\mu,i) = \sum A_{\tau,m}\, \varepsilon(\tau,m|\mu,i) \qquad (2)$$

The indices τ and m label all possible distinct allowed symmetry-adapted distortion modes. τ stands for the possible different mode symmetries, while m (m=1,…n_τ) enumerates the possible different independent modes of a given symmetry. The contribution of each mode is separated into an amplitude $A_{\tau,m}$ and a set of normalized atomic displacements ε within a primitive unit cell, both being *real* quantities. The atomic displacements ε for a given mode $\varepsilon(\tau,m)$ form its so-called *polarization vector*,

that describe its correlated atomic displacements. The set of displacements $\varepsilon(\tau,m|\mu,i)$ within the asymmetric unit of the H-structure, i.e. with $\mu=1,\ldots s$, $i=1,\ldots n_\mu$, define unambiguously the polarization vector of the corresponding symmetry mode (τ,m). The displacements of the remaining atoms within the H-unit cell are obtained by the H space group operations relating these atoms with those in the asymmetric unit. By definition, all modes in (2) separately maintain *at least* the symmetry given by the space group H. Therefore, the displacement of an atom related by an operation $(\mathbf{R}|t)$ of H with atom (μ,i) in the asymmetric unit will be given by $\mathbf{R}\varepsilon(\tau,m|\mu,i)$. The polarization vector $\varepsilon(\tau,m)$ defines the symmetry-adapted mode (τ,m) except for a global amplitude; therefore we will use the terms *mode* and *mode polarization vector* as essentially synonymous.

We choose the polarization vectors of the modes in (1) normalized within a primitive unit cell of the H lattice.

$$\sum \text{mult}(\mu,i)\ |\varepsilon(\tau,m|\mu,i)|^2 = 1 \qquad (3)$$

The symmetry relation just mentioned above permits the reduction of the sum in (3) to the asymmetric unit by considering the multiplicity mult(μ,i) (the multiplicity within a *primitive* unit cell for the space group H) of the corresponding Wyckoff positions. It is important that the normalization in (3) is done with the mode displacements expressed in an absolute length scale. In addition, the basis modes introduced in (1) are chosen orthogonal, so that their polarization vectors fulfill:

$$\sum \text{mult}(\mu,i)\ \varepsilon(\tau,m|\mu,i).\ \varepsilon(\tau',m'|\mu\ i) = \delta_{\tau,\tau'}\ \delta_{m,m'} \qquad (4)$$

This orthogonality is automatically satisfied by modes of different symmetry or irrep, while in the case of modes of the same irrep, a systematic orthogonalization procedure can be applied. Note that this implies that the set of symmetry adapted modes is in general not unique and a certain arbitrary choice must in general be done for any practical calculation.

The set of displacements of each atomic Wyckoff orbit of the parent structure form an invariant subspace for all symmetry operations, so that the symmetry adapted basis can be chosen considering separate basis modes for each atomic Wyckoff orbit in the parent structure, i.e. $\varepsilon(\tau,m|\mu,i)=0$ for all μ except if μ is a specific atom in the asymmetric unit of G. Furthermore, the symmetry constraints of the polarization vector

of a given mode only depends on the type of Wyckoff orbit, so that the set of displacements defining the mode polarization vectors can be chosen identical for all orbits of the same type. Hence, in practice, the index m in the mode basis $\{\varepsilon(\tau,m)\}$ labelling the modes associated with the same irrep, could be decomposed into two labels: one giving the atom representative μ of the set of parent-symmetry related atoms having displacements for this mode, and an additional index for further enumeration of the modes for the same irrep and the same atoms. We will maintain however for simplicity whenever possible a single label m as a short symbolic notation.

For consistency, the maximum number of modes that can be included in (1) coincides with the number of free atomic parameters necessary to describe the H structure in a conventional form, i.e. with the number of (H-symmetry allowed) free parameters in the set of displacements $\{\mathbf{u}(\mu,i)\}$. Expression (1) is then in fact a change of basis in the space of structural parameters describing the structural distortion, i.e. a linear transformation between the atomic parameters $\{\mathbf{u}(\mu,i)\}$, that define the atomic positions in the H-structure and the amplitudes $\{A_{\tau,m}\}$ of the chosen basis of symmetry adapted modes. It is important to stress that the dimension of these amplitudes $A_{\tau,m}$ is length. Therefore, they can be expressed for instance in Angstroms, and the magnitude of different distortion modes present in a distorted structure can be directly compared even if they represent collective atomic displacements of very different kind. The values of the amplitudes $A_{\tau,m}$ can be readily obtained from the set of atomic displacements $\{\mathbf{u}(\mu,i)\}$, once the basis of symmetry-adapted modes $\varepsilon(\tau,m)$ has been chosen, using their orhonormality properties, by a simple scalar product of the distortion with each normalized mode of the basis:

$$A_{\tau,m} = \sum \text{mult}(\mu,i)\ \varepsilon(\tau,m|\mu,i).\mathbf{u}(\mu\ i) \qquad (5)$$

The symmetry of the modes ε is characterized by an irreducible representation (irrep) of the space group G, defining its transformation properties for the operations of the high symmetry group G, plus in general some additional restriction so that the distortion mode keeps the observed symmetry H. In general each distortion mode in (1) maintains in the structure a symmetry which is intermediate between G and H (including H or G themselves). In other words, its *isotropy* group [REF13] is in general a supergroup of H. This implies that the symmetry modes in (1) are restricted to a specific subspace within the representation space associated with their irrep. As this

restriction is always present if we are working with a fixed space group H for the distorted phase, the irrep associated to each mode in (1) can be used as a single label for describing its symmetry, letting implicit the additional restriction forced by the space group H.

The distortion modes with isotropy group equal to H can be called *primary*, while those with isotropy groups given by subgroups of G which are distinct supergroups of H, are usually termed *secondary* [REF14]. A primary distortion mode is sufficient to produce the observed symmetry break between the parent and the observed structure, while secondary distortion modes alone would yield a higher symmetry. Trivial examples of secondary distortion modes are those that maintain the symmetry of the parent structure, i.e. they transform according to the trivial identity irrep. This type of secondary symmetry modes always exist except if all the atoms in the parent structure are located in special positions with all its coordinates forced to special values.

The determination of the amplitudes $A_{\tau,m}$ of the symmetry-breaking modes does not require to know a specific "real" parent structure. Only the amplitudes of modes transforming according to the identity irrep, i.e. those that do not break the space group and are therefore already allowed in the parent structure, depend of the structure-dependent atomic coordinates of the parent structure. A change in the atomic coordinates that are variable under space group G only introduces additional atomic displacements described by modes that transform according to the identity irrep. Therefore, the rest of the distortion, namely the symmetry-breaking distortion remains unchanged for any values of these variable coordinates. Hence, the calculation of the amplitudes $A_{\tau,m}$ of the symmetry breaking distortion modes only requires to know from the high symmetry structure the set of atoms in its asymmetric unit, their type of Wyckoff orbit, and identify in the actual distorted structure the atoms corresponding to these orbits. This identification is necessary for the calculation of the set of displacements $\mathbf{u}(\mu\, i)$, and for this purpose a rough approximate guess of the crystallographic free coordinates of the atoms in the parent structure is in general sufficient.

An ambiguity in the results of the mode decomposition happens if the distorted phase is polar. The set of atomic displacements relating the parent and the distorted structure includes in general a global translation of the crystal that depends on the

(arbitrary) choice of origin of the polar structure. A convenient origin choice is then the one that makes this global translation zero. This would be the choice done in all analyses of polar structures discussed in this article.

It is also very convenient to express the total distortion in terms of the different symmetry components, i.e. as combination of global distortion modes for each of the allowed irreps:

$$\mathbf{u}(\mu,i) = \sum_{\tau} A_\tau \, \mathbf{e}(\tau|\mu,i) \qquad (6)$$

The global amplitudes A_τ are given by $(\Sigma_m A_{\tau,m}^2)^{1/2}$, while the corresponding normalized polarization vector $\mathbf{e}(\tau)$ is determined by the actual linear combination of the symmetry modes $\varepsilon(\tau,m)$, with fixed τ, realized in the structure:

$$\mathbf{e}(\tau|\mu,i) = \sum_m a_{\tau,m}\, \varepsilon(\tau,m|\mu,i) \;\text{ with }\; a_{\tau m} = A_{\tau,m}/ (\Sigma_m A_{\tau,m}^2)^{1/2} \qquad (7)$$

The distortion mode of symmetry τ present in the structure can therefore be described by a global amplitude A_τ and a n_τ-dimensional normalized polarization vector with *components* $\{a_{\tau m}\}$ in the working basis $\{\varepsilon(\tau,m)\}$. The components $\{a_{\tau m}\}$ define the *direction* taken by the observed structure in the n_τ-dimensional space of allowed τ-distortions. The set of components $\{A_{\tau m}\}$ are indeed the components of a n_τ dimensional vector expressed in an orthonormal basis, and any possible τ distortion of the parent structure can be expressed by an amplitude A_τ and the normalized vector $\{a_{\tau m}\}$.

While the polarization vectors $\varepsilon(\tau,m)$ of the symmetry-adapted basis only depend on the symmetry properties of the irrep τ and some arbitrary choice done, the polarization vectors $\mathbf{e}(\tau)$ corresponding to the global τ-distortion is specific for each concrete structure. We shall call these system-dependent symmetry-adapted global distortion modes, present in the distorted structure, *irrep distortion modes*, or simply *irrep distortions*, to be distinguished from the irrep *basis* modes. While the amplitudes A_τ will vary with external perturbations or with changes of the thermodynamic variables of the system, the corresponding polarization vectors $\mathbf{e}(\tau)$ are expected to be system dependent but rather invariant with respect to external fields, and among isomorphic materials. In many cases they can be related with low-energy static normal modes of the system (see section 4), that characterize not only the free-energy minimum realized by the observed phase, but also all the low energy arrangements around this minimum

where the system may *move* with relatively low energy cost.

3. The example of the orthorhombic ferroelectric phase of $BaTiO_3$.

Barium titanate, one of the most studied ferroelectrics [REF15], is known to have a parent phase having Pm-3m symmetry and three consecutive ferroelectric phases of different symmetries as temperature is lowered [REF16, REF15]. In particular, it has an intermediate orthorhombic phase with space group Amm2 in the temperature interval [183K, 273K] [REF16, REF17], which we take here as a first example.

Without including the orthorhombic strain, the space group Amm2 of the orthorhombic phase of BaTiO3 is related with the one of its cubic phase by the transformation c, a-b, a+b; 0,0,0 (footnote explaining the notation). The reported structure (REF18-Kwei et al 1993) of this orthorhombic phase of $BaTiO_3$ is reproduced in Table 1 and shown in Figure 1. The maximum atomic displacement in the distortion with respect to the cubic perovskite phase is smaller than 0.13 A. The number of structural variable parameters in the structure is five, but, as the structure is polar along z, only four of them are really independent. Before performing the mode decomposition, as discussed in the previous section, we shift the origin of the published Amm2 structure along the polar direction in order that the atomic displacements relating both structures do not include a global translation. This shift has already been included in the structure given in Table 1. The atomic displacements relating the Amm2 structure with the parent perovskite structure are then readily obtained from the comparison of the asymmetric unit of the Amm2 structure with the one of the cubic parent phase expressed in the same setting, which is also listed in Table 1.

The Amm2 distortion decomposes into two distortion modes of different symmetry corresponding to the irreps $GM4^-$ and $GM5^-$ [REF19] (T_{1u} and T_{2u} in the notation of … .[REF20]) (footnote: in the following the irreps at the Γ point, will be labelled with the symbol GM, instead of the greek letter, to simplify the notation and to be in accordance with program outputs). Both irreps have Amm2 as isotropy subgroup. The space of the $GM4^-$ distortion has four dimensions while the $GM5^-$ distortion subspace is one dimensional. A basis of five symmetry modes ε (as provided by AMPLIMODES) is listed in Table 2. The polarization vectors of the $GM4^-$ modes for

Ba and Ti are equal and correspond to z displacements of 1Å, while for the oxygens there are two independent $GM4^-$ modes that can be chosen as shown in Table 2. The first of these two oxygen modes involves displacements (in Åmstrongs) of (0,1/√8, 1/√8) for O1 and (0,0,1/√2) for O2, while for the second one, only O1 in the asymmetric unit has a non-zero displacement given by (0,-1/2,1/2). The modes in Table 2 are expressed in relative units with respect to the unit cell of the reference structure for practical purposes.

Using (5) the amplitudes for the 5 modes listed in Table 2 can be calculated. The global amplitudes of the $GM4^-$ and $GM5^-$ distortions result to be 0.165 Å and 0.006 Å, respectively. Hence, the distortion $GM5^-$ is more than 25 times smaller than the polar distortion $GM4^-$. Figure 2(b) depicts the polarization vector of the distortion mode $GM5^-$, which is fully determined by symmetry and is listed in Table 2. It is a non polar mode, totally alien to the ferroelectric instability. Its much smaller weight in the structure is fully consistent with the physical origin of this phase. In fact, the amplitude of mode $GM5^-$ is so small, that its contribution to the actual values of the atomic positions is very close to their standard deviations.

The extremely small value of the $GM5^-$ distortion implies that the structure has some “hidden” non-crystallographic approximate correlation among its atomic coordinates. This can be clearly seen inspecting in Table 3 the polarization vector of the $GM4^-$ distortion mode present in the structure. The five non-zero displacement components in this table are not independent, they are related by three relations: i) absence of global translation, ii) normalization and iii) $GM4^-$ symmetry. More specifically, the $GM4^-$ character of the mode forces the following relation among the components of the oxygen displacements: $\delta y_{O1} + \delta z_{O1} - \delta z_{O2} = 0$. These three relations reduce the number of adjustable free parameters to three, which with the single parameter describing the $GM5^-$ distortion makes the expected total of 4 degrees of freedom in the structure. As the $GM5^-$ distortion mode is very small, the $GM4^-$ symmetry is fulfilled to a good approximation by the total distortion, so that the experimental coordinates of the oxygens satisfy $y_{O1} + z_{O1} - z_{O2} \approx 0$ (for the reported structure $y_{O1} + z_{O1} - z_{O2} = 0.0014 \pm 0.008$). This is an approximate non-trivial non-crystallographic correlation, which is a direct signature of the physical mechanism responsible for the stabilization of this phase, namely the thermal instability of a $GM4^-$

polar mode.

The polar GM4- distortion mode present in the Amm2 structure of BaTiO3 is depicted in Figure 2(b). Although the distortion associated to this phase is usually described as a simple change from the spontaneous polarization (order parameter) from the direction (1,0,0) in the tetragonal phase to (1,1,0) in this orthorhombic one [REF21], it is remarkable that the scheme of correlated atomic displacements is rather complex, and their relation with those associated with the tetragonal ferroelectric phase are not obvious. Indeed the $GM4^-$ distortion mode shown in Table 3 and Figure 2(b) is closely connected with the simple polar distortion along a tetragonal axis present in the tetragonal phase. A quantitative comparison of both distortions can be done if they are considered in the common reference of the parent phase.

4. Hierarchy of modes

The large difference in amplitude of the two distortion modes of different symmetry present in the Amm2 structure of BaTiO3 is a simple example of a property that is expected to happen rather systematically in more complex distorted structures. If a structure is pseudosymmetric, the minimum of the free energy corresponding to this phase in the energy map within the configuration space of the system, should be located in the *proximity* of a saddle point corresponding to the higher-symmetry configuration. The closeness of both points should allow in general a description of this energy minimum by a truncated Taylor expansion around the saddle point associated with the high symmetry configuration. This Taylor expansion expressed in terms of the amplitudes of *normal* static distortion modes, i.e. *diagonal* for the second order terms of the expansion, is the starting point of the Landau theory of structural phase transitions [REF4]. This topological property of the energy landscape around distorted structures is however rather general, and can be used to characterize the structural properties of a distorted structure, independently of the existence or not of a phase transition.

The first terms of a Landau-type expansion around the unstable high-symmetry configuration, with space group G and close to the distorted phase, with space group H (subgroup of G), can be written as:

$$E = Eo + \sum \beta_m \rho_{\Gamma 1,m} + \tfrac{1}{2} \sum \kappa_{\tau,,n} (\Sigma_j \rho_{\tau,n,j}^2) + \ldots \qquad (8)$$

where the mode amplitudes $\rho_{\tau,n,j}$ in (8) correspond to all displacive *normal* modes. These are classified according to their irrep τ (of G), a multiplicity label n, and a third index j for enumerating the different *degenerate* modes associated to the same irrep if this latter is multidimensional, so that several degenerate modes (same stiffness coefficient $\kappa_{\tau,,n}$) exist for the same irrep. All symmetry breaking modes, i.e. all modes not transforming according to the identity representation, do not have linear terms in the energy expansion (8) (the energy of a G configuration is necessarily extremal with respect to G-symmetry breaking distortions). The linear terms in (8) are therefore reduced to the distortion modes allowed in the space group G, i.e. those transforming according to identity irrep $\Gamma 1$, and therefore allowed to be non-zero in the G configuration.

We choose the normal mode amplitudes $\rho_{\tau,n,j}$ in (8) real, and they refer to modes that besides being symmetry-adapted, are also *eigenmodes* of the matrix of second derivatives of the free energy with respect to the atomic displacements. We can say that within the existing freedom in the choice of a symmetry adapted basis, the set of normal modes corresponding to the amplitudes $\rho_{\tau,n,j}$ is a very specific choice that besides being a *symmetry-adapted*, is also a *physically-adapted* basis. These normal modes decompose the space of structural degrees of freedom into collective modes that are energetically independent in the harmonic approximation, their stiffness coefficients $\kappa_{\tau,n,j}$ being a measure of their energy cost. They are eigenmodes of the matrix of atomic force constants. To distinguish this privileged basis of symmetry-adapted modes, we shall call them *eigenmodes*.

At least one of the stiffness coefficients $\kappa_{\tau,n,j}$ in (8) must be negative to make the high-symmetry configuration unstable. The anharmonic terms of lowest order, subsequent to those shown in (8), are then sufficient to explain the off-center minima corresponding to the distorted structures. This implies in general that the observed structural distortion corresponding to these off-center minima will contain mainly low energy eigenmodes. Among them one can distinguish the contribution of primary and secondary eigenmodes, but this distinction adds now a physical condition to the considerations in section 2, where only symmetry properties were involved. Primary eigenmodes are in general those that their condensation is sufficient to explain the observed symmetry break between the parent and the observed phase and are

intrinsically unstable (their stiffness coefficient is negative), while secondary eigenmodes are those that are only present as an induced effect. Within this viewpoint, primary and secondary eigenmodes can be of the same symmetry, their difference being their intrinsic instability or stability.

Secondary eigenmodes, despite having in general positive stiffness coefficients and hence being *hard modes*, appear in the global distortion because they have a symmetry allowed anharmonic coupling with the primary ones of type $\rho_s P^{(n)}(\rho_{p1}, \ldots, \rho_{p2})$, where $P^{(n)}$ is a polynomial term of order n in the amplitudes of the primary eigenmodes, $\rho_{p1},\ldots, \rho_{p2}$. The minimal order n allowed has been called the *faintness index* [REF21-bis]] of the corresponding secondary mode. Neglecting higher order terms, this lowest coupling is sufficient for producing a non-zero amplitude of a secondary mode at the energy minimum, if the primary distortions are non-zero:

$$\rho_s \sim (1/\kappa_s)\, P^{(n)}(\rho_{p1},\ldots, \rho_{p2}) \qquad (9)$$

All secondary eigenmodes present in the distorted phase of space group H are necessarily coupled with the primary ones with terms of this type, i.e. linear in the amplitude of the secondary eigenmode.

Any eigenmode having as isotropy group or invariance group a subgroup of G which is a supergroup of H has in fact such coupling terms, and is allowed in the distorted phase, in accordance with Von Neumann principle [REF22]. Thus this type of coupling is a necessary and sufficient condition for a mode to be present in the distorted structure. Within this perspective, the space group symmetry H associated with the distorted structure, is just an efficient form of defining and introducing the symmetry restrictions that all eigenmodes condensed in the distorted phase should fulfill. The eigenmodes $\{e_E(\tau,n)\}$ compatible with the symmetry H of the distorted phase can be labelled in the same way as we did with a general symmetry adapted basis for an H distortion in eq. (2), and we can express them in terms of the chosen symmetry adapted basis:

$$\mathbf{e}_E(\tau,n|\mu,i) = \sum_m b^{(n)}_{\tau,m}\, \varepsilon(\tau,m|\mu,i) \qquad n=1,\ldots, n_\tau$$

or in a shorter vector notation:

$$\mathbf{e}_E(\tau,n) = \sum_m b^{(n)}_{\tau,m}\, \varepsilon(\tau,m) \qquad n=1,\ldots, n_\tau \qquad (10)$$

or

$$\mathbf{e}_E(\tau,n) = (b^{(n)}_{\tau,1}, b^{(n)}_{\tau,2}, \ldots , b^{(n)}_{\tau, n\tau})$$

The eigenmodes $\{e_E(\tau,n)\}$ can be used as a symmetry and physically adapted basis to describe the distortion modes $\{\mathbf{e}(\tau)\}$(see eq. (6)) present in the distorted structure:

$$\mathbf{e}(\tau) = \sum_n a^E_{\tau,n} \mathbf{e}_E(\tau,n) \qquad (11)$$

According to the arguments above, if τ is the symmetry of a primary mode, the decomposition (11) will be dominated by the unstable primary eigenmodes within the set of eigenmodes $\mathbf{e}_E(\tau,n)$ of the same symmetry τ. The rest of *hard* eigenmodes of the same symmetry τ will contribute in general with much smaller amplitudes, described in a first approximation by eqs. of type (9). As can be seen in eq. (9) secondary eigenmodes with larger stiffness constants are expected to have smaller amplitudes in the distortion, although the strength of the coupling with the primary eigenmodes plays a role may alter this general trend.

If τ corresponds to a symmetry only associated with secondary eigenmodes, the static distortion of this symmetry present in the structure is expected to be much smaller than the primary one, because of its typical dependence on a power of the primary mode amplitudes. The relative weight of the different eigenmodes of the same symmetry will be essentially governed by eq. (9), i.e their relative amplitudes are approximately inversely proportional to their stiffness, and proportional to their coupling with the primary modes.

Summarizing, the decomposition of a distorted structure in terms of symmetry modes is expected to evidence quite different weights or amplitudes for the different irrep distortions present in the structure. Distortion modes that are *primary* from the symmetry viewpoint will have much larger amplitudes and can be identified in a good approximation with the mode(s) that is(are) intrinsically energetically unstable and are the origin of the observed structure, with small corrections due to presence of frozen secondary modes of the same symmetry. In the case of ambiguity with respect to the possible irrep associated with the primary distortion, a comparison of their respective amplitudes is in most cases sufficient for their identification, and therefore for identifying the mechanism underlying the stabilization of the phase.

5. An improper ferroelectric: gadolinium molybdate

An improper ferroelectric is a ferroelectric phase where its polar distortion responsible of the spontaneous polarization is a secondary mode [REF23]. The symmetry of an improper ferroelectric cannot therefore be explained by the presence of a polar distortion. This latter is usually not intrinsically unstable in the parent paraelectric phase and its appearance in the distorted phase is induced by its coupling with a primary unstable non-polar distortion mode. The spontaneous electric polarization in these materials is usually very small, compared with those in proper ferroelectrics, as expected from the secondary role of the polar mode in the stabilization of the phase.

Gd2(MoO4)2 is a well known improper ferroelectric [REF24,REF25]. Its ferroelectric phase (see Figure 3) has space group Pba2, with a duplication of the unit cell (transformation a-b, a+b, c; 0, ½, 0) with respect to its parent structure of symmetry P-42$_1$m, which is stable above 160 C. The maximum atomic displacement in the displacive distortion is of the order of 0.4 A. Figure 4 shows the graph of maximal subgroups relating the space groups of both phases, with indication of possible irrep distortion of P-42$_1$m yielding these symmetries. As shown in the graph, we must expect in the Pba2 phase three distortion modes. A primary one yields directly the observed symmetry and corresponds to the (physically irreducible [REF26]) irrep M2+M4, associated with the point M (1/2,1/2,0) at the border of the Brillouin zone. A second mode at the centre of the Brillouin zone with symmetry given by irrep GM3, only breaking the symmetry up to the intermediate subgroup Cmm2, is also symmetry allowed and will also be present as a secondary distortion mode. This second mode is polar and should be responsible for the spontaneous polarization of the Pba2 phase. Finally, there can also be a fully symmetric GM1 distortion keeping the parent symmetry. The number of independent symmetry modes corresponding to these symmetries is 22 and 15, for the M2+M4, GM 3 subspaces respectively, while the subspace of GM1 distortions has 14 dimensions, in accordance with the number of free atomic parameters already present in the parent P-421m structure. In other words, the determination of the M2+M4, GM3 and GM1 stortions requires 22, 15, and 14 parameters, respectively, so that their total number is 51, in accordance with the number

of free parameters in a conventional description of the Pba2 structure (REF25).

A summary of the mode decomposition of the Pba2 experimental structure reported in (REF25) is given in Table 4. Again here the primary distortion is dominant, its amplitude being more than one order of magnitude larger than the secondary distortion GM3. In a very good approximation the structure can be described considering only the M2+M4 and the GM1 distortions, i.e. with a significant decrease of 30% in the number of positional parameters compared with a conventional description.

Tables S1 to S4 in the supplementary material (footnote : supplementary material….) completes the mode description of the Pba2 structure of GdMoO in a form following crystallographic conventions. The Table lists a Pba2 asymmetric unit, with the atomic positions corresponding to the reference parent phase of higher symmetry [REF25]. For this asymmetric unit, Tables S2, S3 and S4 list the atomic displacements in relative coordinates defining the normalized polarization vectors of the GM1, M2+M4 and GM3 distortion modes present in the structure. This information together with the mode amplitudes in Table 4 is sufficient for obtaining, just by adding up the three sets of displacements, the atomic coordinates of the asymmetric unit, that define the observed Pba2 structure in a conventional form. Put in this form, these tables give also information of the pattern of correlated atomic displacements associated with the modes of different symmetry intervening in the distortion. One can see in Table S3 that the mode GM3 involves mainly atomic displacements on the plane xy, while the displacements along z, which are the only ones with polar character, are typically one order of magnitude smaller. In fact, considering the very small amplitude of this GM3 distortion, its z displacements, except in the case of the Mo atoms, are practically zero within their experimental error. Jeitschko (REF25) already pointed out that the estimated value of the spontaneous polarization in this structure considering nominal charges was smaller than its standard deviation.

The fact that the GM3 atomic displacements along z are practically negligible does not mean however that the atoms remain static along this direction. They displace indeed along this direction, but following essentially the symmetry pattern corresponding to the mode M2+M4, as shown in Table S2. This means that the total structure has some approximate hidden non-crystallographic atomic correlations which

are satisfied within experimental resolution, similarly as it happens in the orthorhombic phase of BaTiO3 discussed in section 3.

6. Domains and equivalent structures.

It is well known from domain theory [REF 54] that, for a given distorted structure with symmetry H <G, there is a series of equivalent structures, which are distinguishable when refered to the common reference parent structure, i.e. the so-called domains, variants or twin-related structures.

If the left coset decomposition of H with respect to H is given by:

$$G= H +g2H + \dots gnH \qquad (12)$$

with n being the index of the subgroup H, the application of the coset representatives 1, g2,…gn on the distorted structure H produces n equivalent structures associated with the expected n distinct domain configurations. The space group symmetry of these n equivalent structures are given by the space groups Hn, equivalent to H, given by gnHgn-1. Within the picture of the configuration energy map discussed in section --, it means that there are n equivalent energy minima around the saddle point associated with the parent phase, giving place to the multistability or degeneracy of the distorted phase, with the possibility of switching processes through external fields between the different equivalent energy minima.

The mode decomposition as formalized in the previous sections is restricted to a specific orientation (and origin shift) between the subgroup H and G, given by the transformation matrix (P,p) relating the two space groups. Hence the details of the decomposition refer to a specific subset of configurations among the domain-like equivalent ones mentioned above. This means that among the possible equivalent orientations and origin relations between the low and high symmetry structures a choice must be done, and the concrete expressions for the polarization vectors of the irreps distortions will depend on it. The amplitudes of the irrep distortions are however independent of the choice of subgroup H, among the equivalent ones.

In many cases some coset representatives gn , are such that

$$gnHgn^{-1} = H \qquad (13)$$

so that the symmetry of the corresponding domain equivalent configuration is described by the same space group H. In these cases, the mode decomposition of this equivalent configuration may yield a change of sign of some of the distortion amplitudes, or equivalently a change of sign of the corresponding normalized polarization vectors.

In general, if a distorted structure is described by a set of irrep distortions with amplitudes {At1, At2, …Atp} , and gn is a coset representative in (12) such that eq. (13) is satisfied without any change of orientation of the space group H, then an equivalent domain-related structure is obtained considering the same polarization vectors for the irrep distortions and the transformed amplitudes through the action of the space group operation, i.e. {t1(gn)At1, t2(gn)At2, …,tp(gn)Atp}, where t1(gn) is necessarily +1 or -1 according to the tranformation properties of each amplitude given by the corresponding irrep. The value of +1 or -1 of the factors ti(gn) are in general correlated. Those of the secondary modes can be directly derived from those of the primary modes through the relation (9) connecting the amplitudes of the secondary distortions to the primary ones. This equation considers the lowest coupling terms among primary and secondary distortions, but the resulting sign correlation is a symmetry property that is maintained at any level of approximation.

If the distorted structure contains a single primary distortion, the mode decomposition of the domain related configuration will yield a primary distortion with opposite sign, while secondary distortions will change sign or not depending on their faintness index (see section --) being odd or even. If, on the contrary, there are several primary distortions (with different irreps) in the structure, in most cases more than two domain equivalent configurations for the same fixed subgroup H will exist (i.e. more than one coset representative gn will fulfill eq. (13)), and the different domains will be distinguished by independent uncorrelated changes of sign of the different primary distortions, while secondary distortions will have their signs correlated to those of the primary ones according to eq. (9) (footnote: in some cases the action of all “lost” symmetry operations, gn , on a given primary irrep distortion cannot be reduced to a factor +1 and -1, and in these cases, the distortion will have a fixed sign in all domains with the same H).

The subset of equivalent domain configurations corresponding to a fixed H <G

and obtained by the allowed changes of sign of the primary distortions (and correlated ones of the secondary ones) correspond to different equivalent crystallographic descriptions of the same structure, obtained by means of transformations belonging to the euclidean normalizer of the group H extended to the specialized metric that the unstrained lattice obtained by the transformation of the lattice of the supergroup G may have (REF 26-bis).

We can consider the two structures discussed above as simple examples of the above considerations. In the case of the Amm2 phase of BaTiO3, there are 12 equivalent distorted structures of this symmetry with respect to the Pm-3m perfect perovskite. They correspond to the 6 different distinct subgroups Amm2 of Pm-3m belonging to the same conjugacy equivalence class, and associated with 6 different orientations of the rotational operations of the group Amm2 with respect to the Pm-3m setting. Once chosen one of these subgroups by means of the transformation c, a-b, a+b; 0,0,0, the distorted structure can have two equivalent configurations related by the lost inversion operation, which can be taken as the coset representative fulfilling eq. (13). The inversion operation changes the sign of both the primary polar distortion of symmetry GM4- and the secondary one GM5-. Hence the two equivalent structures can be described by opposite amplitudes (AGM4-, AGM5-) and (-AGM4-, -AGM5-), while maintaining the polarization vectors. As in a mode decomposition the amplitudes are usually chosen positive by definition, the change of sign will be reflected in the polarization vectors considered, which would be opposite in both configurations. The correlated switch of the sign of both distortions is consistent the faintness index of the GM5- distortion, which is 3, as can be easily checked using the program INVARIANTS of the package ISOTROPY (REF). Hence, in the lowest order, the amplitude AGM5- is proportional to AGM4-^3. Note that this means that although an external electric field only couples linearly with the polar distortion mode GM4-, it can not only switch this primary , but also the secondary non-polar one GM5- through the anharmonic coupling among the two distortions.

In the second example, gadolinium molybdate, the index of the subgroup is 4, and we can chose as coset representatives the following operations (1|0 0 0), (-4| 0 0 0), (1|1 0 0), (-4|1 0 0) . The rotoinversion operation -4 changes the orientation of the Pba2 space group, and corresponds to another choice of the transformation matrix (P,p). On the other hand, the lost translation (1|1 0 0) transforms the distorted structure into its

so-called antiphase domain. This translational operation only changes the sign of the primary mode, while keeping the signs of the two secondary distortions GM4 and GM1. Thus, once fixed the transformation (P,p) relating both structures, and maintaining the same polarization vectors, the two alternative domains for this compound correspond to the distortion amplitudes (AM2M4, AGM4, AGM1) and (-AM2M4, AGM4, AGM1). These correspond to two equivalent structures related by the operation of euclidean normalizer of Pba2, (1|1/2,1/2,0). Therefore the amplitude of the primary distortion can have any sign, while the sense of the secondary polar mode GM4, and hence of the spontaneous polarization is fixed. This latter can however be switched by means of an electric field, but this corresponds to the action of the coset representative (-4|0 0 0), and therefore also implies a tranformation of the polarization vector corresponding the primary distortion M2M4 according to the action of the point group operation -4, not being reducible to a mere change of sign. This means that the reversal of the spontaneous polarization along the pseudotetragonal z-axis through the action of an electric field will be accompanied by the tranformation by the operation -4 of the non-polar M2M4 atomic displacements described in Table S2, which are mostly on the plane xy.

Below we will show further examples where two primary distortion modes are active and the set of variant or domains through correlated changes of the distortion amplitudes is more varied.

7. A strongly distorted ferroelastic: Leucite.

We consider now the structure of leucite. This mineral, with formula $KAlSi_2O_6$, is tetragonal (I41/a) at room temperature, but becomes cubic (Ia-3d) above approximately 940 K (see REF27 and references therein). An intermediate phase in a very narrow temperature interval with space group $I4_1/acd$ has also been reported [REF 28,27]. There is a group-subgroup relation between the room temperature I41/a and the high-temperature symmetry Ia-3d, but as can be seen in Figure 5 the displacive distortion relating both phases is very large. The connected framework of SiO4 and AlO4 tetrahedra suffer a strong rearrangement when passing from the cubic to the tetragonal configuration with a collapse of the cation stuffed trigonal channels of the cubic phase. In this case the maximum atomic displacement is of the order of 1 A, a value

considerably larger than in the examples discussed above. Nevertheless, we will see in the following that despite the large magnitude of the distortion, it still can be rationalized in terms of modes. The temperature evolution of the structure includes the variation of two distortion modes with different symmetry, and as a consequence having quite different temperature behaviour.

The number of atoms per primitive unit cell is the same in both phases, and therefore only modes at the Brillouin zone centre, i.e. modes keeping the lattice periodicity, are involved in the distortion. It suffices to introduce the experimental structures [REF27] of the two phases in the mentioned program AMPLIMODES, together with the transformation matrix relating the settings of the two space groups (a,b,c;1/2,0,0), to obtain the amplitudes and the specific features of the symmetry distortion modes present in the tetragonal phase. A scheme of the group-subgroup tree relating the parent and distorted symmetry is shown in Figure 6. There is a primary mode (irrep GM4+) which yields the observed symmetry break between the two phases, plus a secondary mode (irrep GM3+) with a higher isotropy subgroup (I41/acd), and the usual full symmetric distortion mode (irrep GM1+). The 30-dimensional configuration space of the I41/a structure (30 independent atomic coordinates define the structure) divides among these three distortion subspaces of 16, 10 and 4 dimensions, for GM4+, GM3+ and GM1+, respectively. Their amplitudes at room temperature result to be 4.61, 1.82 and 0.41 A. As expected the primary mode is significantly larger, although not in such strong proportion as in the other examples discussed above.

Palmer et al. [REF27] made a series of high-resolution powder neutron diffraction measurements of leucite as a function of temperature below and above the phase transition around 940K, and have reported structural models for the material at various temperatures. It is illustrative to analyse these structures in terms of modes and observe the temperature behaviour of the three distortion modes active in the tetragonal phase. Their amplitudes follow a well-behaved smooth temperature dependence, shown in Figure 7(a). Note that apart from the structures determined above room temperature, the study in [REF27] also determined the structure at 4K. Even the amplitudes corresponding to this isolated point at very low temperature agree with the smooth curves suggested by the high temperature data. The available points for the amplitude of the GM4+ distortion mode has been fitted to a continuous function, following the typical law of an order parameter of a discontinuous phase transition [REF2]. What is

especially remarkable is that the curve fitted to the GM3+ amplitudes is just the square of the curve used for the GM4+ amplitudes, with only a scale factor having been fitted. Hence, we are observing a primary component in the structural distortion behaving as the primary order parameter, while a second one, weaker but significant, varies its amplitude as the square of the amplitude of the primary distortion, as expected from a secondary mode with faintness index 2 (see section 4). It should be stressed that in general for each individual atomic position the contributions of the two modes superpose, and therefore the simple law underlying the thermal evolution of the structure shown in Figure 9(a) is usually not directly observable in the thermal changes of single atomic coordinates or atomic distances.

One can also follow the temperature variation of the polarization vectors of the two distortion modes. The value of their scalar product with the one corresponding to the structure at 4 K can be used to monitor its change. One can see in Figure 7(b) that the polarization vectors of both modes are in general rather temperature invariant. This means that in each distortion mode the atoms follow well defined invariant correlated relative displacements, the temperature variation being essentially reduced to their global amplitude. This is specially true for the primary mode. For this mode except for the points closer to the transition the dot product maintains values larger than 0.99, and does not decrease in any case below 0.97. The polarization vector of the secondary mode GM3+ has a more significant variation, but is also quite small, except close to the transition.

The approximate invariance of the polarization distortion modes can be understood in the light of the discussion presented in section 4. If we consider only the lowest anharmonic coupling of the secondary normal modes to the primary one and assume them essentially temperature independent as done in Landau theory, the secondary distortion mode minimizing the free energy will be formed by a linear combination of secondary normal modes that will be kept invariant for changes of the temperature and the amplitude of the primary normal mode. For the primary distortion mode something similar happens, except that it is expected to have an overwhelming proportion of the primary normal mode. Hence, deviations of the ideal invariance due to higher order anharmonic coupling terms are expected to be smaller.

One may argue that the remarkable “rigidity” of the polarization vectors of the

distortion modes is due to the fact that they correspond to rigid unit mode (RUMs) [REF29] of the tetrahedral framework in the leucite structure. Both distortions can be indeed considered RUMs for the framework of AlO4 and SiO4 tetrahedra. But the primary GM4+ distortion includes a significant relative displacement of the K cations, and its participation in the mode polarization vector is also invariant. We will see below other examples where connected framework of rigid units can not be considered, but nevertheless the property of the approximate invariance of the polarization vectors of the distortion modes is maintained, even between different compounds.

In Figure 7(b) one can see that the polarization vectors of both the primary and the secondary distortion mode have their largest variation close to the phase transition. We have observed this behaviour also in other systems. It is not clear if this is a genuine structural feature or an experimental spurious effect coming from the intrinsic difficulty of the measurements in the proximity of a phase transition. It is clear that the experimental uncertainty on the polarization vector increases as the mode amplitude of the mode decreases. The relative decrease of the amplitudes does not seem however sufficient to explain this systematic variation of the polarization vectors when the transition is approached. On the other hand, it has been shown in many cases that the primary distortion mode well below the transition agrees nearly full percent with the primary normal mode. It can be then hardly understood that this agreement should deteriorate somehow as the system approaches the transition. The simple model explaining this correlation is in principle expected to be more appropriate for smaller distortions. Therefore we speculate that the significant variations of the distortion polarization vectors close to the transition points is an indication of a poorer determination of the structures in these conditions.

It is remarkable that the intermediate phase of symmetry $I4_1/acd$, which has been proposed for a small temperature interval above 900 K, just before reaching the parent cubic configuration, would correspond to a primary distortion of symmetry GM3+, while a distortion of this symmetry is also present at room temperature, but only as a secondary induced distortion, as shown in Figure 7(a). It would be rather strange to have a distortion of this symmetry acting as a primary (unstable) mode only at higher temperatures. The mode decomposition of the $I4_1/acd$ structural model at T=923K of [REF27] yields an amplitude for this distortion of 0.86 A, also shown in Figure 7(a). This value is clearly at odds with the temperature behavior of the amplitude of the

GM3+ distortion in the I41/a phase, which shows a fast but smooth tendency to zero at a temperature around 900K. The polarization vector of the GM3+ distortion mode in the P41/acd structural model is in fact very different from the one corresponding to the I41/a phase, indicating that it a quite different type of distortion despite having the same symmetry.

A primary mode responsible of a distorted phase is expected to be intrinsically unstable, with temperature acting as stabilizing factor, so that in general, its disappearance at lower temperatures is usually caused by its incompatibility with new stronger instabilities of different symmetry. This is not the case here, since the phase I41/a produced by the primary GM4+ distortion mode is compatible with any GM3+ distortion. Of course, there can be exceptional cases of reentrant transitions, but this intermediate P41/acd phase would be even a more exceptional case, since the GM3+ distortion present would disappear when the system enters the I41/a phase, although it is fully compatible with this symmetry. We can therefore conclude that most probably the structural model proposed for this claimed intermediate phase is not correct. Furthermore, the behaviour of the amplitude of GM3+ distortion below 900K shown in Figure 7(a) suggests that no intermediate phase of such symmetry exists.

7. Hexagonal perovskites ABX_3

There is a considerable number of ABX_3 compounds which crystallize in the so-called hexagonal perovskite (2L) structure or slight distorted modifications of it. A representative of the parent hexagonal perovskite structure, with P63/mmc symmetry, underlying these structures is CsNiCl3 [REF 46]. For smaller A cations, the structure is usually distorted at room or lower temperatures, and polar configurations are rather common, producing ferroelectric phases [REF 47]. If the B cations are magnetic magnetically ordered phases also exist at low temperatures, and multiferroic properties combining ferroelectricity and magnetic ordering are in principle possible. We will see here that it is very illustrative and illuminating to analyze and compare the structures of this family, doing a systematic mode decomposition with respect to the ideal hexagonal perovskite configuration.

We first consider a representative of the family, namely the compound KNiCl3

[REF48-especifica]. In the parent P63/mmc phase Ni, K and O occupy positions 2a, 2d and 6h. It has a ferroelectric phase at room temperature with space group P63cm with a triplicated unit cell (a+2b, -2a-b, c; 0 0 0). A mode analysis of this phase was done "by hand" in REF 49. We present here its mode decomposition as obtained directly with AMPLIMODES, using the parameterization introduced above. The graph of maximal subgroups and irreps, relating the symmetry of the ferroelectric phase with that of the parent phase, is shown in Figure 8. One can see that there is a primary active irrep with wave vector (1/3,1/3,0) and label K3 (footnote: in REF49 the label used was K4. Here we maintain the labels provided by AMPLIMODES in accordance with the convention of ISOTROPY AND ISODISPLACE which is essentially that of Miller and Love ?? [REF..]) and two secondary active irreps associated with two intermediate subgroups. The K1 distortion also corresponds to a wave vector (1/3,1/3,0), so that it produces the cell multiplication, but maintains the point group of the parent phase, while the second distortion, GM2- at the Brillouin zone center, keeps the parent lattice and is the polar mode responsible of the spontaneous polarization in the distorted phase.

From Figure 8 it can be deduced that the symmetry break from the parent phase to the room temperature structure could take place by means of two quite different mechanisms. The most obvious one would be a single phase transition with K3 acting as active primary irrep, and distortions GM2- and K1 appearing as secondary effects. But one could imagine a more complex symmetry breaking mechanism, with GM2- and K1 being primary unstable modes, and producing in general two phase transitions, with an intermediate phase of symmetry P63cm or P63/mmc, depending on which of the two first becomes zero as temperature is increased. This alternative mechanism has been in fact considered as a possibility in the case of YMnO3, which has a similar symmetry relation with its parent space group as KNiCl3, although both parent and distorted structures are quite different [REF 50].

In the case of KNiCl3, as in YMnO3 [REF-51, 52] , however, the mode decomposition in terms of the three symmetry breaking components K3, K1 and GM2- of the structure of KNiCl3 leaves little room for speculation. Their respective amplitudes (in A) are listed in Table 5. The much larger amplitude of the K3 antiferrodistortive distortion is a clear indication that it can be identified with the primary order parameter of this phase, and it can be further inferred that K1 and GM2- are induced secondary effects. The material is then a ferroelectric of improper character.

Figures 9 and 10 illustrate the polarization vectors of the three types of distortions intervening with so different amplitudes in the total observed distortion. The primary K3 distortion involves displacements of the columns of NiCl6 octahedra along the z-axis, with the two internal columns displacing in opposite direction to the one at the origin. The magnitude of the displacement of this latter doubles the one of the internal columns. This non-crystallographic correlation introduced by the K3 symmetry is patent in the polarization vector listed in Table 7. The splitted Ni1 and Ni1_2 atoms within the asymmetric unit of the distorted structure move in opposite directions along z, with a ½ relation among its displacements. The same relation exist among the displacements of the two Cl sites. But the table shows an additional correlation between the displacements of the Cl and Ni sites, namely their displacements within each column of NiCl6 octahedra are practically equal within experimental resolution, so that the distortion mode involves global displacements of the NiCl3 colums as rigid units. This correlation in the polarization vector of the primary K3 distortion is not forced neither by symmetry, nor by a strong rigidity of the Ni positions within the octahedra. In the observed structure in fact the Ni atoms clearly displace relatively to their surrounding Cl6 octahedra and approach along the c axis one of the two Cl3 triangles forming the octahedron. But these Ni displacements are not part of the K3 distortion, they follow a pattern according to the GM2- symmetry, as shown in Figure 6(b). In this GM2- distortion, all Ni atoms move in phase with the same amplitude, while the Cl atoms displace also in phase with similar amplitude but in the opposite sense. The GM2- distortion is completed with the displacements of the K atoms outside the octahedral columns, which move in the same direction as the Ni atoms. Hence we have a polar distortion with cations and anions moving in opposite senses, and therefore susceptible of producing a significant polarization, as observed experimentally [REF 47]. The mode decomposition also evidences that the displacement off-center of the Ni atoms within the NiCl6 octahedra is not part of the fundamental distortion (normal mode) that is unstable. This means that most probably these off-center shifts of the Ni atoms are not intrinsically favourable in energy terms, in contrast with the pure K3 distortion.

It should be stressed that by definition a distortion mode with a non-zero wave vector cannot induce any polarization, and only polar modes at the Brillouin zone center, as the GM2- , can be considered at the origin of any spontaneous polarization and can linearly couple with an external electric field. This is sometimes overlooked

and in the present compound has led to speculations about possible ferrielectric properties [REF-53-japoneses]. From Figure 6 one can clearly see that the polar displacements of the GM2- distortion are fully homogeneous. Ferrielectricity can therefore not be supported by the experimental structure, and the confusion probably originates in the erroneous consideration of the dominating K3 distortion pattern (with opposite displacements of the octahedral columns) as the source of the spontaneous polarization.

The secondary distortion K1, although quite small, seems to be significant within experimental resolution. As shown in Figure 10 and Table 7, this distortion concerns displacements of the chlorine and potassium atoms on the xy plane. The chlorine atoms in consecutive Cl3 triangles along the octahedral NiCl3 columns rotate in opposite senses around the z axis, while the displacements of the K atoms between the columns move in a sense consistent with the expected steric hindrances caused by the chlorine displacements.

The faintness index (see section …) of the secondary distortion K1 is 2, while that of the polar mode GM2- is 3 (footnote: this can be readily checked using the program INVARIANTS from the package ISOTROPY (http://stokes.byu.edu/isotropy.html and REF…). Hence, the sign of the amplitudes of the secondary distortions are bound to that of the primary mode, according to the proportionality laws:

A_{K1} proport. A_{K3}^2 (14)

A_{GM2-} proport. A_{K3}^3

This means that an equivalent structure or domain (see section 6) will be given by the following changes in the signs of the amplitudes: (-AK3, AK1, -AGM2-). This is very important to compare the mode decomposition of similar or closely related structures. Table 8 compares the mode decomposition of KNiCl3 with those of other ABX3 P63cm structures considered isomorphic, namely TlFeBr3, RbMnBr3, BaMnO3 and TlCoCl3 (footnote: the inorganic crystal structure database [REF] contains a few additional cases with vanadium as B cation, and RbTiI3 extracted from REF 60, but unfortunately in these models the z coordinate of two atoms (instead of one) were a priori fixed in the refined model, and therefore the structural models cannot be considered realistic). The

amplitudes of the three symmetry-breaking distortions are listed, and their polarization vectors are compared through their dot product with the one of KNiCl3. One can see that in the five compounds the distortion K3 is predominant and has within experimental resolution the same bidimensional polarization vector, which means that in all cases the octahedral BX3 columns displace as rigid bodies, including the B cations inside the BX6 octahedra. The polar distortion GM2- has however clear differences. Although the GM2- distortion in TlFeBr4 is essentially the same as in KNiCl3, the positive sign of their dot product is inconsistent with the change of sign observed in the primary distortion K3. This means that in TlFeBr3 the polar displacements of the A, B cations and X3 columns along z displayed in Figure 9(b) have opposite senses, with respect to the sense taken by the primary K3 distortion. In other words, an equivalent K3 distortion in both compounds would produce a spontaneous polarization in opposite directions. This must be taken with caution. It may happen that indeed the anharmonic coupling between similar K3 and GM2- distortions in the two compounds has opposite signs, but another reason could be that one of the two models corresponds to a local false minimum in the refinement process. Indeed, it has sometimes been reported in distorted structures false minima in the least square minimization corresponding to changes of sign of some of the irrep distortions modes present in the actual structure (REF 61).

The sign of the dot products of the polarization vectors of the GM2- distortions in the other three compounds is consistent when compared with the dot product of the K3 mode. However, the three distortions differ significantly from the one of KNiCl3, as its dot product is only of the order of 0.7-0.8. This difference can be further assessed comparing the atomic displacements associated with the distortion mode in each case. Table 9 shows the polarization vector of the GM2- distortion mode of TlCoCl3. One can see that in contrast with KNiCl3, the B cations displace along z in the same sense as the chlorine atoms, and with nearly the same amplitude, so that in this case the octahedral BCl3 columns essentially move as rigid units in the polar distortion. The very small off-center shift of the B cations within the octahedra is close to the experimental error and in fact in the opposite direction to the one observed in KNiCl3. We can expect the spontaneous polarization to be much weaker than in KNiCl3.

The GM2- distortion in BaMnO3 and RbMnBr3 is very similar to the one of TlCoCl3. This can be seen in Table 8, where the alternative dot product with respect to

the polarization vector of this distortion in TlCoCl3 is also shown. One can observe therefore, that despite the similarities among the structures, a clear difference exists in the secondary polar distortion of the materials, between the Ni and the Mn or Co compounds.

The very weak marginal K1 distortion has much larger variations between the compounds. As its amplitude is much smaller than the other two irrep distortions, its polarization wave vector is expected to have a larger error. In some of the compounds its amplitudes is so small, as in TlCoCl3, that it could considered as negligible; its polarization vector however is rather close to the one of KNiCl3 (see Tables 7 and 9), with A cations and Cl anions displacement being correlated in a similar form (see Figure 9). In some of the other compounds the polarization vector is quite different and the sense of the displacements of the A cations relative to those of the X anions can change.

One can then summarize that the primary distortion mode is quite robust and transportable from one material to another, while the secondary distortions can vary considerably. In some cases this could be due to false local minima in the refinement process, while in others it can happen because of genuine changes in the scheme of harmonic and anharmonic couplings among the atomic displacements between different compounds. In any case, secondary modes have much smaller amplitudes and are bound to be worse determined. A look at the structure decomposed into modes can be very useful both to avoid the traps of false refinement minima, and to compare structures, where the differences appear mostly in changes of the secondary distortions, which although quite weak can be fundamental for the macroscopic properties of the material.

Some of the studies on these compounds have indicated that the alternative symmetry P-3c1, instead of P63cm could also used to refine the experimental data of the distorted structure with similar reliability factors, and in some cases the experimental data was not sufficient to distinguish between the two models and only an arbitrary choice between the two models could be done (REF57, REF58). In fact, as easily checked with SYMMODES [REF] or ISOTROPY[REF] this alternative symmetry for the distorted phase would also correspond to a distortion K3 as primary mode, and K1 as secondary. The difference with the P63cm symmetry break would be associated with a change in the direction of the order parameter K3 in its two-

dimensional irrep space, i.e. a different (orthogonal) linear combination of the two independent modes of this symmetry. This would be sufficient to change the symmetry to P-3c1, and cancel the possibility of having a secondary polar distortion. The fact that the structure of this secondary polar distortion, only present under the hexagonal symmetry, is quite comparable in all the compounds (see table 8), is a significant factor that favors the P63cm model as the most plausible one.

Another illustration of the insight that the mode decomposition can provide is the comparison of the structure of RbMnBr3 at 80K, which has its mode decomposition summarized in Table 8, with the structure of the same compound at 1.7K, reported in the same work (REF 57). The amplitudes of the three irrep distortions of K3, K1 and GM2- symmetries are at this lower temperature 0.53, 0.15 and 0.14, respectively, to be compared with the ones listed in Table 8 for the structure at 80K. The distortion amplitudes have increased as one would expect, but their polarization vectors have some clear inconsistent variation. Their dot product with those at 80K give 0.9998, -0.90 and 0.996, respectively. Hence, the distortion K1 keeps its internal structure similar to the one at 80K, but has its sign switched, while the other two distortions are practically invariant except for its amplitude increase. As discussed above, the K1 distortion has its sign fixed by that of the primary mode, and a change of sign of this distortion describes a non-equivalent structure. Therefore, we have here most probably another example of a defective structural model caused by a secondary refinement minimum with some of the irrep distortions switched. As the amplitude of the K1 mode is significantly larger at 1.7K, the incorrect sign of this distortion is most probably the one at 80K. This could also been inferred from Table 8, where the decomposition can be compared with the one of KNiCl3.

Further consideration requires the hexagonal ABX3 compounds that exhibit a distorted structure of even lower symmetry. KTiCl3, KTiBr3 and KTiI3 are reported to have a distorted hexagonal 2H perovskite structure with space group P63. The three structures have been obtained from single crystal X-ray diffraction and reported in a recent publication [REF 62]. The reliability factors are however rather poor, the weighted R factor being 0.10, 0.15 and 0.16 for KTiCl3, KTiBr3 and KTiI3, respectively. Clearly, the structural model for KTiCl3 is much more reliable than for the other two compounds. One can do a mode decomposition of the three structures similar to the one done for the P63cm compounds. The transformation matrix relating the

lattice and origin of these P63 compounds with the one of the hexagonal 2H perovskite is the same as for the group P63cm. Hence the space group of these compounds is a subgroup of the P63cm observed in the compounds discussed previously. Figure 11 shows the graph of maximal subgroups relating the parent and distorted symmetries in this case. The irrep distortions permitted by the P63cm symmetry are enlarged with new irrep components associated with other intermediate symmetries. The most important point evidenced by Figure 11 is the fact that there is no single irrep distortion that can produce the symmetry break between the parent and the distorted symmetries, i.e. the distortion present in these P63 phases must have more than one primary distortion. From Figure 11 it is clear that at least two distortions corresponding to two different irreps are necessary to explain the symmetry break. There could be many pairs of irrep distortions which could be responsible of the observed symmetry P63, but assuming that the irrep K3 is also in these compounds a primary distortion, the second primary mode could only be either GM2+, K4 or K2. The presence of any one of these three distortions together with the K3 distortion would be sufficient for explaining the observed P63 symmetry. The mode decomposition of these three structures summarized in Table 10 permits to identify the distortion GM2+ as the searched second primary distortion. It is clearly the dominant component of the distortion superposed to those yielding the P63cm symmetry, in the three compounds. This distortion is represented in Figure 12. Its polarization vector is fully determined by symmetry, as only one basis symmetry mode is involved. It is a rotation of the octahedral BX3 columns around the z direction. As a primary distortion, a switch of the sense of these rotations independently of the sign of the other primary distortion K3, yields an equivalent configuration. Figure 11 shows that the secondary distortions K2 and K4 must be induced by the simultaneous presence of both primary modes, as their isotropy subgroups are not supergroups of any of the two primary symmetries P63cm or P63/m, but of their intersection P63. Indeed, using the module INVARIANTS from ISOTROPY (REF) it can checked that the lowest coupling of distortions of symmetry K2 and K4, with both primary modes, and responsible of the induction in the distorted phase are AK3AGM2-AK2 and $AK3^2AGM2$-AK4, respectively. Both distortions are therefore sensitive to the sign of the GM2- distortion, while only K2 would also switch with a change of sign of the K3 distortion.

The K3, K1 and GM2- distortions present in these three P63 structures are

compared in Table 10 with those of the P63cm phase of KNiCl3. In the case of KTiCl3, the coincidence of the polarization vectors of the three distortions is striking, despite the quite different amplitudes. To be stressed is the correlated change of sign of the K3 and GM2- distortions, corresponding to an equivalent twin related configuration. On the other hand, the mode decomposition of the other two compounds, with much worse reliability factors, points to where the problems of these structural models could be. While the polarization vector of the primary mode K3, given by a single parameter, is essentially the same as in KNiCl3, the secondary ones have much larger relative amplitudes than in KTiCl3 and their three dimensional polarization vectors have *erratic* changes of sign, not even consistent between the two. If KTiI3 and KTiBr3 are compared, their distortions GM2- and K1 are very similar but with their signs switched, and not corresponding to equivalent twin related configurations. Probably these structures also correspond to false minima associated with switched secondary modes.

The mode decomposition of these P63 ABX3 structures also helps to infer the probable temperature behaviour of these compounds. If, as usual, they adquire the parent symmetry P63/mmc at high temperatures, one can expect the existence of an intermediate P63cm phase after the second primary mode GM2+ is thermalized. One cannot discard of course a single first order phase transition with both order parameters becoming zero simultaneously, but in most cases two active irreps imply two successive symmetry breaks.

9. Distorted pseudocubic perovskites. Sequence of phase transitions

There are many ABX3 structures having as parent structure the cubic perovskite with space group Pm-3m. Depending on the so-called Goldsmidt or tolerance factor which somehow indicates the misfit of the sizes of the three intervening ions, different distorted structures exist, and the cubic parent phase is often reached at high temperatures after following some sequence of phase transitions. For these simple structures with rather rigid BX6 octahedra, a mode description is quite simple; many normal modes are fully determined by symmetry and can be identified with tilts or RUMs [29] of the framework of octahedra. A good deal of the distortions present in these compounds can in fact be described as tilting schemes of the BO6 octahedra, and have been rationalized from this viewpoint [REF30,31,32]. The more general approach

of a mode description has also been considered and investigated [REF 33,34]. It is not the aim of this section to review such extense subject. We only want to present a few cases within this family, as further examples of the power of a systematic mode decomposition.

i) SrZrO3

Let us consider the very well studied case of SrZrO3, which has at room temperature a distorted perovskite structure with Pnma symmetry [REF35, 36 and references therein], which is typical of many ABX3 compounds having a too small A cation to stabilize the cubic configuration. The cubic perovskite structure is only attained in this compound above 1340K. The setting of its orthorhombic Pnma space group is related with the supergroup Pm-3m corresponding to its parent structure by the transformation: a+c, 2b, -a+c; 0,0,0. The distortion involves mainly correlated tiltings of the ZrO6 octahedra, i.e. RUMs of the octahedral framework (see Figure 13), with a multiplication of the unit cell by a factor 4. This implies the presence of a considerable number of distortion modes of different symmetry, compared with the examples considered above. On the other hand the number of free atomic coordinates is quite limited. Figure 14 shows the graph of maximal subgroups connecting the two space groups and, if existing, the irrep yielding these intermediate symmetries as isotropy subgroups [REF7]. It can be seen that distortions with three different wavectors M (½ ½ 0), X (0 ½ 0) and R (½ ½ ½), at the border of the cubic Brillouin zone will be present in the Pnma structure. Furthermore, the graph shows that the Pnma symmetry of this phase is not an isotropy subgroup of Pm-3m, i.e. this symmetry cannot be attained with a single primary mode. At least two primary modes are necessary. In other words, the Pnma phase cannot be generated by a single mechanism or a single unstable mode of the cubic configuration, but at least two different normal modes must be active. In the language of Landau theory, the phase Pnma should be the result of the condensation of two order parameters. These order parameters are in general expected to be thermalised and become zero at higher temperatures, but each one independently, producing two phase transitions. Thus, one can expect from this simple symmetry relation regarding the parent and distorted space groups, the probable presence of an intermediate phase before the system reaches the cubic perovskite.

From the graph in Figure 14 one can establish the different possible primary

distortions that may be relevant. One has to look for pairs of isotropy subgroups which have as intersection the observed space group Pnma. There are many possibilities. Any pair of the distortions indicated in the graph, except for the pair of the two M modes or of the pair of two R modes would be sufficient to explain the observed Pnma symmetry.

A mode decomposition of the experimental structure at 20C [REF35] clearly indicates which are the ones relevant. Table 11 lists the amplitudes of all the distortion modes, and one can clearly see that two distortion amplitudes are much larger, namely those of the distortion modes R4+ and M3+, with the one for R4+ being significantly larger. A scheme of the five distortion modes participating in the Pnma structure can be seen in Figure 15, and their polarization vectors are listed in Table 12. The two primary distortion modes are tilting modes of the octahedra with a single symmetry mode involved, and therefore fully determined by symmetry. The secondary mode X5+ however involves both oxygen and Sr displacements, and despite implying some distortion of the octahedra it has a significant non-zero amplitude. The two remaining secondary distortion modes are very weak. The M2+ is zero within experimental resolution, while the R5+ distortion although very small is present in the structure, and mainly involves displacements of the Sr atoms along the orthorhombic z direction.

Distortion modes of symmetry R4+ and M3+ are therefore the two dominant primary distortion modes underlying the Pnma structure of SrZrO3. An analogous symmetry mode decomposition in other compounds shows that this in fact happens in most of the distorted Pnam perovskites, with again the R4+ distortion being somehow stronger in most cases. In this simple case, these primary modes are defined in one-dimensional spaces (see tables 11 and 12), and their polarization vectors are fully determined by symmetry, corresponding to simple so-called *tilt systems* of the octahedra [REF 30,33]. Only their amplitudes are variable, and and for small values they are linearly related with the corresponding tilt angle.

The identification of these tilt sytems as the two primary modes, with a symmetry given by an irrep of the parent space group Pm-3m, is an information directly obtained from the structure, which is very valuable to infer possible transition sequences, and general trends in the whole family. In fact, as pointed out in previous literature [REF 33], the instability of the perovskite cubic configuration with respect to

RUMs of symmetry R4+ and M3+ underlies many of the distorted phases with various symmetries observed in perovskites. The R4+ RUM modes correspond for instance to the well known (three fold degenerate) instability present in SrTiO3 which competes with the ferroelectric one [REF37 and references therein], and yields for this compound at low temperatures a tetragonal phase with I/4/mcm symmetry (footnote: the irreps labels are those of CML??, also used by ISODISPLACE and ISOTROPY [REFs], but do not necessarily coincide with those used in other studies [REF 34]. Unfortunately, even keeping a fixed specific choice of notation, the irrep label may change depending on the origin choice in the parent structure. For instance, if the origin is chosen at the site of the Sr atom instead of the Zr, the irrep label of the distortion R4+ would change to R5-). Both irreps R4+ and M3+ are three-dimensional and the distortion and symmetry realized in SrZrO3 corresponds to specific directions within the space of each representation indicated symbolically in Table 11. An extended general explanation of the meaning of specific directions of a distortion mode within the irrep space and their relation with the isotropy subgroup, can be found in [REF 38, 33]. In the present case, changing the direction within the irrep space, means in general a change of the axis around which the tilts of the octahedra take place, with a consequent change of the resulting (isotropy) space group. For instance, the possible symmetries for a R4+ distortion are given by the following isotropy subgroups (footnote: they can be obtained with ISODISPLACE [REF] and they are also listed in [REF 33]):

I4/mcm, (a+b, -a+b ,2c; 0,0,0) , (a,0,0)

Imma, (a+c, 2b, -a+c; 0,0,0), (a,a,0)

R-3c, (-a+b, -b+c, 2a+2b+2c; 0,0,0) , (a,a,a)

C2/m, (-2c, 2b, a+c; 0,1/2,1/2), (a,b,0)

C2/c, (-a+2b-c, -a+c,a+c; 0,1/2,1/2), (a,a,b)

P-1, (b+c, a+c a+b; 0,0,0), (a,b,c)

Where the last row indicates for each case the direction of the distortion in the irrep

space, in the notation of [REF37].

For a given R4+ instability of the cubic perovskite, the realization of one or other space group of the above list depends on the anharmonic terms in the free energy function discussed in section 4, which creates the anisotropy of the energy map in the three-dimensional subspace defined by the R4+ unstable three-fold degenerate distortion modes. Usually, because of the smoothness of the energy map the energy minima will correspond to high symmetry directions within the energy map [REF 39] . These energy minima can change with temperature and a sequence of first order phase transitions then happens, with symmetry changes between different isotropy subgroups of the same irrep. This is observed for instance in CeAlO3 where only R4+ modes act as primary modes with a phase transition sequence:

I4/mcm --- Imma ---- R-3c ----- Pm3m

for increasing temperature [REF40, 32bis], corresponding to changes of direction of the R4+ order parameter (distortion) according to the list of isotropy subgroups above. This is fully analogous to the consecutive dicontinuous phase transitions taking place in BaTiO3, due to changes of the direction of its spontaneous polarization, which are directly related with changes of direction of its polar GM4- distortion within its three dimensional irrep space (see section 3).

In the case, of SrZrO3, the R4+ distortion corresponds to the direction (a,a,0) with symmetry Imma. It is namely a combination of two equal tilts around the [1,0,0]p and [0,0,1] p cubic axes, which is equivalent to a tilt around the oblique direction [1,0,1]p, i.e. around the x direction of the orthorhombic setting (see Figure 12).

As the R4+ distortion is clearly much stronger than the M3+ distortion, one can infer that this latter will be thermalized at lower temperatures leaving a phase with only R4+ as primary distortion. If the direction of the R4+ distortion mode does not change one can predict a phase transition into a phase with Imma as space group, which can in principle be continuous. If temperature is further increased subsequent transitions corresponding to changes of direction of the primary R4+ distortion mode may happen, until the cubic phase is finally reached. And indeed this what happens in SrZrO3, with a reported transition sequence [REF36]:

Pnma --- Imma --- I4/mcm --- Pm-3m

Therefore, the relative weight of several primary distortion modes in a distorted structure can give important clues concerning its behaviour at higher temperatures. We can crosscheck this by comparing the mode decomposition of SrZrO3 with the analogous phase of NaTaO3 [REF41], also shown in Table 11. In this compound the amplitude of the R4+ distortion is about 20% smaller, while the M3+ distortion is of the same magnitude. Although the R4+ distortion is still larger, its amplitude is much closer to the one of M3+. In this case the transition sequence is quite different:

Pnma --- Cmcm ---- P4/mbm --- Pm-3m

The mode decomposition of these high temperature phases is shown in Table 13. It can be seen that the Cmcm phase is also the result of the presence of the two distortion modes with irrep symmetry R4+ and M3+, but the R4+ distortion has changed its direction, so that now its isotropy subgroup is P4/mcm. Its amplitude is now significantly smaller than the one of the M3+ distortion. One can then infer that the next phase P4/mbm must corresponds to a phase caused only by the presence of the M3+ distortion, with the R4+ distortion thermalized at a lower temperature than the M3+, the opposite of what happens in SrZrO3.

The M2+ distortion, which distorts the BX6 octahedra (see Figure 15 and Table 12) is practically negligible both in SrZrO3 and NaTaO3, but can have important amplitudes in the Pnma phase of perovskites with Jahn-Teller ions. The local symmetry of the octahedral distortions associated with this mode correspond to the one induced by the local Jahn-Teller effect [REF63]. Table 11 shows the mode decomposition of LaMnO3 [REF64], where the presence of a significant M2+ distortion is patent, in contrast with the previous examples. Despite its compatibility with the symmetry produced by the two primary dominant distortions R4 and M3+, the M2+ distortion in Jahn-Teller Pnma perovskites act as a third primary mode instead of as a secondary induced distortion. In fact this additional primary mode usually introduce a new phase transition corresponding to its independent condensation. As the Pnma symmetry is compatible with the distortion, this additional Jahn-Teller transition would not represent any symmetry change in a structure with both R4+ and M3+ already frozen, and a isosymmetrical Pnma --- Pnma transition takes place, with a conspicuous increase of the amplitude of the M2+ distortion acting as a non-symmetry breaking order parameter. This is what happens for instance in LaMnO3 at room temperature at 750K [REF64].

8. Distorted structures as commensurate modulated structures. Mode decomposition vs. superspace description

Although not fully equivalent, the description of commensurately distorted structures in terms of symmetry-adapted distortion modes is closely related with the alternative approach of considering these structures as commensurately modulated and the use of superspace symmetry [REF 42, 43]. Displacive distortion modes are in fact displacive modulations with wave vectors associated with their corrresponding irrep. Thus, in the previous example of SrZrO3 there are modulations with wavevectors (½ ½ 0), (0 ½ 0) and (½ ½ ½).

In the description of a commensurately distorted structure as a modulated phase a set *primary* modulation wave vectors are defined and the distortion is described as a superposition of harmonics for this set of wave vectors. The symmetry is given by a superspace group, which defines the correlations and symmetry restrictions that the atomic displacements must have for each of these harmonics. In the case of incommensurate structures the number of harmonics is unlimited, but in practice, a hierarchy exists and the first harmonics are expected to be dominant, so that the expansion can be truncated. In a commensurate case, the number of possible harmonics is finite, and a hierarchy between first and higher harmonics also exists, so that in some cases the highest harmonics can be neglected. Under these premises, the program JANA [REF67], for instance, is adapted to treat and refine any commensurately distorted tructure with up to three independent primary modulation wave vectors, using the superspace formalism.

In simple cases, a mode decomposition in terms of irrep distortion modes and a decomposition with modulation harmonics under a postulated superspace group are fully equivalent, i.e. each irrep distortion corresponds to a specific harmonic in the modulation. The secondary modes can in general be identified with higher order harmonics in the superspace description. This happens when the average space group in the superspace group is the one of the parent structure and a single primary wave vector exists, so that the modulation is one-dimensional. In more complex cases, the two methods may have some differences in the decomposition of the global distortion. In general, if the unit cell of the distorted phase is much larger than the parent one, a mode decomposition would not bring much benefit to what is already provided by the

superspace approach, and would be somehow less efficient, as the structure of the polarization vectors are trivially given by the modulation wave vector. On the other hand, for supercells in the distorted phase which are only a small multiple of the parent phase, and involve modulations along several directions, the mode approach is much more convenient.

We illustrate these considerations with some examples. Let us consider first the simple case of the triclinic structure of NbS3. van Smaalen [REF65] showed that the triclinic structure of this compound with space group P-1 could be described and refined as a modulated structure with modulation wave vector (0 ½ 0), with respect to a basic monoclinic structure having space group and a unit cell with half the volume. The structure could be refined satisfactorily introducing a single harmonic in the modulation, which implied to use a smaller number of parameters than a conventional refinement in the triclinic space group P-1. The reason for this can be clearly seen in the mode decomposition of the structure, if determined in a conventional form (REF66), which is summarized in Table 14. The decomposition has been done with respect to a virtual parent P21/m structure symmetrising the experimental one, so that the GM1+ distortion has been minimized to cero. One can see that the symmetry breaking distortion has two components: a strong distortion Z1 with wave vector q= (0, ½ , 0) yielding the observed symmetry, and a much weaker secondary distortion GM2+ at the Brillouin zone center, with an amplitude more than one order of magnitude smaller. This secondary mode also breaks the binary symmetry, but maintains the lattice of the parent phase. Its weakness is another example of the hierarchy of distinct irrep distortions in distorted structures, which has been discussed all over this paper. In the superspace description this secondary distortion corresponds to a second harmonic with wave vector 2q, which for this commensurate case is formally equivalent to (0,0,0), but that the superspace description treats separately [REF43]. Hence, a superspace refinement of the structure considering only sinusoidal modulations done in REF65 is fully equivalent to a refinement within a model with only the primary distortion Z1 as part of the symmetry breaking distortion, with the distortion GM2+ forced to have cero amplitude.

Let us consider now a more complex case in the much-studied ferroelectric phase of K2SeO4. This structure has been both analyzed as a modulated phase [see REF44 and refs therein] and in terms of irrep distortion modes [REF45]. It is a

commensurate Pna21 structure, with a triplication of a parent Pnma unit cell, which is the consequence of the lock-in of the modulation wave vector q=alpha a* of a previous incommensurate phase into the value alpha=1/3. It is then natural to describe this structure as a one-dimensional modulated phase with the same superspace group as the incommensurate phase, but with a commensurate wave vector, as was done in [REF44].

We can however also apply the mode decomposition explained above. To use AMPLIMODES we only need to introduce the Pnma (parent) and Pna21 structures, and the tranformation relating both groups: -3a, c,b; 0 0 0. The results are summarized in Table 15. As expected, we have a dominant component for the irrep SM2, with wave vector (1/3,0,0) (footnote: it important to stress that even keeping a fixed standard for the labelling of the irreps (here consistent with ISOTROPY and REF (Cracknell….), the irrep labels may change for different equivalent choices of the wave vector representative. One should also take into account the dependence of the irrep label mentioned above on the choice done for describing the parent structure). This prevailing SM2 distortion is the primary unstable mode that comes from the incomensurate phase through the lock-in of the wave vector. This primary distortion corresponds to the first harmonic of the modulation in the incommensurate phase and determines the superspace group symmetry governing the symmetry properties of all additional harmonics [REF65]. There is also a weaker distortion with the same wave vector but different irrep, namely SM3. This secondary distortion can be identified with the second harmonic in a modulated description. For a wave vector q=(1/3,0,0), the second harmonic distortion has the same wave vector as the first harmonic, but in the superspace approach, as in the previous case, it can be treated as a distinguishable second harmonic of the modulation functions if we use the superspace group symmetry of the preceding incommensurate phase. The symmetry properties of the atomic displacements described by the irrep SM3 are then equivalent to those introduced on the second harmonic modulation by this superspace group. Similarly the additional GM4- distortion is the polar distortion responsible of the spontaneous polarization and ferroelectric properties in this commensurate phase, and can be identified with a third harmonic in the atomic modulations [REF 45, 68]. In this example, it is noticeable that the two allowed secondary distortions have smaller but significant amplitudes, so that a satisfactory direct refinement of the structure using either modes or superspace modulation functions requires the same number of positional parameters as a

conventional refinement.

As a third example we take the mode decomposition of the ninefold commensurately modulated phase of thiourea (SC(NH2)2). This structure is an intermediate lock-in phase sandwiched within the extense range of an incommensurate phase [REF 69]. The parent non-modulated structure has Pnma symmetry, and the modulation wave vector is q=1/9 b*, with therefore a ninefold multiplication of the unit cell. The structure has been refined both as an incommensurately modulated structure using the superspace approach [REF 70] and as a conventional superstructure [REF 71]. The two models were shown to be approximately equivalent [REF 43] (see below). Table 16 illustrates the features of the structure refined as a conventional superstructure when decomposed in irrep distortions (the hydrogen positions have not been included). A distortion with symmetry given by the irrep DT4 with a wave on the line DT (0,beta,0) of the Brillouin zone with beta=1/9 is dominant. The amplitudes of the additional distortions are between 10 to 20 times smaller so that it can be clearly identified as the primary mode. Note that the four symmetry compatible irrep distortions have as isotropy subgroup the observed space group, and therefore from symmetry argument any of them could be the primary distortion. In this case the primary character of the distortion with q=1/9 b* can only be derived from the comparison of the amplitudes of the different irrep distortions, in contrast with the preceding case. Also, in contrast with K2SeO4, here all irrep distortions have different wave vectors corresponding to distinct harmonics of the primary one. Depending on the parity of the irrep wave vector, the small representation associated with the distortion modes changes from DT4 to DT1. It is noticeable that the secondary third order harmonic with wave vector 3q=(0,1/3,0), of the same symmetry as the primary distortion, has a larger amplitude than the second one, with a different symmetry. This third harmonic is responsible for the soliton like form of the atomic modulations in the superspace description [REF 69,43]. The modulated refinement in [REF 69] was done using only harmonics up to 3rd order for describing the atomic modulations. This means the neglection of a possible fourth order harmonic, which in the mode decomposition corresponds to the weaker DT1 distortion with wave vector 4q= (0, 4/9, 0). Table 16 shows that in the model refined as a conventional superstructure the amplitude of this distortion, although very small, is larger than its standard deviation and therefore significant. This difference is at the origin of the small differences between the positions

in the two models, shown in REF 43.

It is interesting to compare the description done of each harmonic modulation in the two approaches, showing how in this case, the mode parameterization discussed here becomes inefficient and highly redundant, compared with the superspace approach. Table 17 shows the polarization vector of the primary DT4 distortion. To be noticed how the distortion is in practice restricted to displacements along the x and z directions, although the DT4 symmetry does not forbid displacements along the y direction. However, the description of the distortion mode is quite redundant. The three cations S, C and N have a single independent site in the parent unit cell and are splitted into 5, 5 and 9 independent sites, respectively, in the ninefold structure. To describe the distortion mode it is necessary to give the mode displacements for all atoms in the large asymmetric unit of the distorted phase with 19 atoms. In these 19 atomic displacements the trivial correlation between consecutive parent unit cells along the modulation direction coming from the mode wave vector is inextricably entangled with the non trivial one coming from the actual DT4 character of the irrep. In contrast, the superspace approach only requires giving explicitly the three amplitudes that define the first harmonic of the modulation function for the three independent atoms in the asymmetric unit of the parent phase [REF 70]. The sinusoidal function so defined, together with the modulation wave vector is sufficient to describe the displacements of the equivalent atoms in the nine consecutive parent unit cells forming the superstructure unit cell, while the correlation according to irrep DT4 with those atoms that are symmetry related by rotational operations in the parent phase is automatically introduced by the applied superspace group [REF 72].

In REF 71 where a conventional refinement was performed two distinct models (models 1 and 2) within the Pnma space group were reported. The authors could not decide between the two models, although clearly different, as both gave equal reliability factors. It was pointed out in REF 43 that this uncertainty was due to the invariance of the diffraction pattern for a global phase shift of the atomic modulations when described as a modulated structure in superspace, and the two models corresponded to the two distinct different choices of the global phase of the modulation, namely pi/18 and -pi/18 (or their equivalents by shifts of 2p/9). This close relation between the two models is also reflected in their mode decomposition, as shown in the following. Up to now we have only discussed the mode decomposition model 1. While

the tranformation relating model 1 with the used parent structure (-a, -9b, c;0 0 0) did not require any origin shift, a proper comparison of model 2 requires, if the parent structure is kept unchenged, to add an origin shift (0 ½ 0). This means that in the case of mode 1 the inversion centre at the origin is mantained, but not the one at (0 ½ 0), while in model 2 the reverse happens. Table 18 presents the resulting mode decomposition of model 2. One can see that the amplitudes of the four irrep distortions coincide with the ones of model 1, if their standard deviations are taken into account. The difference between the two models appears however, in the column that lists the direction taken by the irrep distortion within the irrep space. In this case the irrep is bidimensional and a two dimensional vector (a, za) gives the direction with respect to a chosen orthonormal basis. This fixed direction is related with the fixed global phase of the modulation forced in a modulated description of the structure. Comparing Table 16 and table 18 one can see that the angle phi=arccot(z) for the primary distortion is -2pi/36 for model 1, while it is 2pi/36 in model 2, and therefore we can directly relate this angle with the modulation global phase of the modulated description. In the modulated description the global phases of the secondary harmonics are multiples of the primary modulation in accordance with their order. The directions listed in Tables 16 and 18 fullfill analogous relations. If we call phi1 the angle arccot(z) for the primary mode in each model, the corresponding phases for the secondary modes with wave vectors 2q, 3q, and 4q are (pi/2 -2phi1), 3phi1 and (pi/2-4phi1), respectively. The meaning of this angle depends on the basis chosen in the irrep space. Thus, the third harmonic with the same symmetry DT4 as the primary distortion fulfill directly the expected phase correlation, while for the even modes, due to some with DT1 symmetry, the complementary angle appears due to a change in the setting used (or a coupling with factor i numero imaginario PENDIENTE DE COMPROBAR)

As a final example to illustrate and evidence clearly the similarities and differences of both approaches we consider phase GaII of the element Ga under pressure, which to our knowledge is the most extreme case achieved in parameter reduction when describing a superstructure as a modulated structure within the superspace formalism. This phase of symmetry C2221 [REF 74], stable between 2 and 10 GPa, has a very large unit cell with 14 symmetry independent Ga atoms, but it has been shown to be a simple commensurately modulated structure of a Fddd structure with only a symmetry independent atom in the Wyckoff position 8a (1/8, 1/8, 1/8) [REF

73]. The superspace group describing the symmetry properties of the modulation was found to be Fddd(00gamma) 0s0, with gamma= 9/13. Hence the modulation wave vector was chosen (0 0 9/13) and the conventional unit cell is multiplied by 13, with respect to the virtual Fddd parent structure. Within the superspace approach the number of possible harmonics for the single atomic modulation required to define the full structure is 25. But the structure could be satisfactorily described with only three harmonics, which meant a reduction from 38 to 4 positional parameters, when passing from a conventional crystallographic description to a modulated one. The transformation relating the setting of the Fddd parent structure with the experimental one [REF 74] can be chosen as a,-b,-13c; -1/8 ,1/8,-3/8. The maximum atomic displacement in the distortion relating both structures is of the order of 0.8 A and its mode decomposition is summarized in Table 19. The number of possible irrep distortions is 25, in accordance with the number of allowed harmonics in the superspace description, but the irreps involved have only 13 possible wave vectors of type n/13 c*, with two different possible small irreps for each of them except for n=13, which corresponds to a special point Z at the brillouin zone border and only an irrep is compatible. The irrep distortions with n odd all have as isotropy subgroup the observed symmetry and are from this viewpoint possible primary modes, while the even modes are all secondary, with higher isotropy subgroups. The amplitudes obtained for the 25 symmetry components in the distortion evidences the dominant role played by the LD3 distortion with wave vector q= 9/13 c*, in accordance with the superspace description. This LD3(9/13) distortion is clearly the primary distortion, being more than one order of magnitude larger than the rest of components, except for two additional irrep distortions, which can be identified with a second and a third harmonic. Indeed, the LD4[1/13] distortion with a considerable amplitude has a wave vector equivalent to 3q, while LD2[8/13] can be identified with a second harmonic with wave vector 2q equivalent to -8/13c*. These three irrep distortions correspond therefore to the three first harmonics, which were considered sufficient in [REF 73] to describe the structure. In general, for each wave vector n/13 c* two irrep distortions exist with symmetries LD3 and LD4 for odd terms and LD1 and LD2 for even terms, except for the case n=13, with a single irrep Z1. Each of these irrep distortiond corresponds to one of the harmonics used in the superspace description. A modulation harmonic of order m (m=2,...,25) in the superspace description is in fact a distortion with wave vector qm= 9m/13 c* which can be changed to an equivalent wave vector qn= n/13 c* (n=1,…,13)

through a reciprocal lattice translation 2p c* (p integer): qn= qm + 2p c* or –qm+2p c*. This change implies also to change the small irrep associated with the wave vector, depending on the parity of p, so that for n odd, it changes from LD3 to LD4, depending on p being even or odd, while for n even, the change is from LD1 to LD2 for p even to odd. This property can be derived from the form of the irreps of space groups, and their labelling through a wave vector representative and a small irrep, which depends on the chosen wave vector [REF-irreps]. Thus, for instance the LD3[1/13] distortion can be considered a 23rd harmonic, its wave vector being q23= 23*(9/13) c* = -(1/13)c* + 8(2c*) with p even, while LD4[1/13] corresponds to the third order harmonic with q3= 3(9/13)c*= (1/13)c*+2c*, and p odd. Following these rules the correspondance between the 25 harmonics of the superspace description and the 25 irrep components of the mode decomposition can be done. This is given in the first column of Table 19. It can be clearly seen here the equivalence between the two approaches, and the more efficient way the superspace approach can deal with the symmetry constraints present in each harmonic. The choice of the superspace group implies a decision about which of the 25 irrep distortions is the primary modulation. Once a superspace group is assumed, the superspace symmetry automatically introduces the symmetry properties of each harmonic, and a rough hierarchy in their importance is implicitly assumed. The mode decomposition, on the other hand, does not assume a priori any predominance among the 25 irrep components, and one has to define and indicate explicitly one by one the symmetry properties of each possible irrep distortion present in structure. Only the actual mode decomposition and the values of the distortion amplitudes for a given structure will allow to identify if there exist a primary prevailing distortion. Even if a primary distortion has been a priori identified from experimental results, the identification of the secondary modes of lowest order among all possible irrep distortions, susceptible of having more weight in the total distortion, require non-trivial consideration, as shown above.

Although the structure of GaII, as stressede in REF 73, is clearly very well described by the three first modulation harmonics, indicated in Table 19. There are some additional distortion amplitudes, which seem to be significant (being clearly larger than their standard deviations). It remarkable that even for these smaller components the underlying hierarchy for odd harmonics coming from the primary mode is observed; a fact that supports the consistency of these smaller components of the reported structural

model. Thus, as shown in Table 19, the next two irrep distortions with the largest amplitudes of 0.16 and 0.12 A can be identified with the 5^{th} and 7^{th} modulation harmonic. On the other hand, the secondary modes with n even, except the second harmonic, have amplitudes that can be taken as zero, considering their standard deviation.

(PENDIENTE DE CALCULAR CON AMPLIMODES INCLUYENDO ERRORES, para modificar texto

8. Mode Analysis in ab-initio calculations. A natural basis of symmetry modes

8.0 SPS

8.1 $SrAl_2O_4$

8.2 $Bi_4Ti_3O_4$

9. Conclusions

Tables

Table 1. Asymmetric unit of the Amm2 structure of BaTiO3 at 190K according to [REF18], compared with the reference structure Pm-3m parent structure expressed in the same setting. The unit cell of this latter is used for translating the atomic displacements into absolute values. Note the splitting of the oxygen orbit in the orthorhombic space group. The origin of the published Amm2 structure has been shifted along z so that the atomic displacements relating both structures do not include a global translation.

Amm2 phase (a=3.9828, b=5.6745, c=5.6916)	Pm-3m phase (reference structure) (a=4.006000, b= 5.665339, c=5.665339)
Ba 2[a] 0.0 0.0 0.00508	Ba 1a 0.0 0.0 0.0
Ti 2b 0.5 0.0 0.5221(5)	Ti 1b 0.5 0.0 0.5
O1 4° 0.5 0.2561(3) 0.2394(4)	O 3c 0.5 0.25 0.25
O2 2° 0.0 0.0 0.4941(6)	O 0.0 0.0 0.5

Table 2. Basis of symmetry distortion modes of the parent structure Pm-3m of BaTiO3, restricted to the isotropy subgroup Amm2. The atomic displacements for the polarization vector of each mode is expressed in relative units with respect to the reference unit cell, indicating only the displacements of the Amm2 asymmetric unit (see Table 1). Modes are normalized within a primitive unit cell of the Amm2 structure. The modes are labelled by their irrep, the atom representative of the parent Wyckoff orbit involved in the mode and an additional numerical index in the case of the existence of several independent modes for the same irrep and the same atom.

mode		δx	δy	δz
GM4-,Ba	Ba	0.000000	0.000000	0.176512
GM4-, Ti	Ti	0.000000	0.000000	0.176512
GM4-,O,1	O1	0.000000	0.062406	0.062406
	O2	0.000000	0.000000	0.124813
GM4-,O,2	O1	0.000000	-0.088256	0.088256
	O2	0.000000	0.000000	0.000000
GM5-,O	O1	0.000000	-0.062406	-0.062406
	O2	0.000000	0.000000	0.124813

Table 3. Polarization vector (normalized to 1 A) of the polar GM4- distortion mode present in the orthorhombic phase of BaTiO3. The mode is defined using the asymmetric unit of the reference structure and unit cell indicated in Table 1. Displacements are expressed in relative units. This polarization vector corresponds to the combination of the four GM4- basis vectors described in Table 2. with amplitudes 0.17, 0.76, -0.25, and -0.57 (in the same order as in Table 2).

Atom	δx	δy	δz
Ba	0.0000	0.0000	0.0308
Ti	0.0000	0.0000	0.1339
O1	0.0000	0.0349	-0.0665
O2	0.0000	0.0000	-0.0317

Table 4. Summary of the decomposition in symmetry-adapted distortion modes with respect to its P-421m parent structure of the Pba2 structure of Gd2(MoO4)2 at 190K reported in (Jeitschko 1972).

K-vector	Irrep	Direction	Isotropy Subgroup	Dimension	Amplitude (Å)
(0,0,0)	GM1	(a)	P-42_1m (113)	14	0.15
(0,0,0)	GM3	(a)	Cmm2 (35)	15	0.07
(1/2,1/2,0)	M2M4	(a,b)	Pba2 (32)	22	1.62

Global distortion: 1.63 Å

Table 5. Summary of the decomposition in symmetry-adapted distortion modes with respect to its P63/mmc parent structure of the P63cm structure of KNiCl3 (REF48). As reference a symmetrized idealized P63/mmc structure has been used (see Table 6).

K-vector	Irrep	Direction	Isotropy Subgroup	Dimension	Amplitude (Å)
(0,0,0)	GM1+	(a)	P6_3/mmc (194)	1	0.02

(0,0,0)	GM2-	(a)	P6_3mc (186)	3	0.22
(1/3,1/3,0)	K1	(a,0)	P6_3/mcm (193)	3	0.07
(1/3,1/3,0)	K3	(a,0)	P6_3cm (185)	2	1.70

Global distortion: 1.72 Å

Table 6: Reference structure for KNiCl3 corresponding to its parent hexagonal P63/mmc phase in the P63cm setting of its distorted structure

185
11.795007 11.795007 5.926000 90.000000 90.000000 120.000000
5

Ni	1	2[a]	0.000000	0.000000	0.000000
Ni	1_2	4b	0.666667	0.333333	0.000000
K	1	6c	0.333334	0.000000	0.750000
Cl	1	6c	0.160000	0.000000	0.250000
Cl	1_2	12d	0.826667	0.333333	0.250000

Table 7: Polarization vectors of the K3, K1 and GM2- distortions present in the P63cm structure of KNiCl3. The asymmetric unit is that of Table 6. Displacements are given in relative units with respect to the reference unit cell (Table 6). Polarization vectors are normalized to 1A.

	K3			K1			GM2-		
Atom	δx	δy	δz	δx	δy	δz	δx	δy	δz
Ni1	0.0000	0.0000	-0.0482	0.0000	0.0000	0.0000	0.0000	0.0000	-0.0311
Ni1_2	0.0000	0.0000	0.0241	0.0000	0.0000	0.0000	0.0000	0.0000	-0.0311
K1	0.0000	0.0000	0.0000	0.0288	0.0000	0.0000	0.0000	0.0000	-0.0437
Cl1	0.0000	0.0000	-0.0489	-0.0078	0.0000	0.0000	0.0000	0.0000	0.0249
Cl1_2	0.0000	0.0000	0.0244	-0.0029	-0.0137	0.0000	0.0000	0.0000	0.0249

Table 8: Comparison of the mode decomposition of the P63cm phase of different ABX3 compounds. The third column indicates the dimension of each distortion subspace. For each compound the first column shows the amplitude of each irrep distortion, while the second indicates the value of the scalar product of its polarization vector with that of the corresponding distortion in KNiCl3. The structural models have been taken from REF 48 (KNiCl3), REF 55 (TlFeBr3), REF 56 (RbMnBr3), REF 57 (BaMnO3 at 80K), REF

58 (TlCoCl3).

	Isotropy Subgroup	D	KNiCl3		TlFeBr3		RbMnBr3		BaMnO3		TlCoCl3	
			ampl.	prod.	ampl.	prod.	ampl.	prod.	ampl.	prod.	ampl.	prod.
GM2-	P6_3mc (186)	3	0.21	1 0.70	0.36	0.98 0.53	0.39	0.77 0.994	0.14	-0.74 -0.997	0.16	0.70 1
K1	P6_3/mcm (193)	3	0.07	1	0.10	0.70	0.02	0.67	0.04	-0.55	0.007	-0.89
K3	P6_3cm (185)	2	1.70	1	1.15	-0.9997	1.72	1.0000	0.42	-0.9999	1.02	0.9999

Table 9: Polarization vectors of the K3, K1 and GM2- distortions present in the P63cm structure of TlCoCl3. The asymmetric unit is equivalent to that of Table 6. Displacements are given in relative units with respect to the experimental unit cell (11.86 11.86 5.98). Polarization vectors are normalized to 1A.

(Combinar con Table 7???)

	K3			K1			GM2-		
Atom	δx	δy	δz	δx	δy	δz	δx	δy	δz
Co1	0.0000	0.0000	-0.0488	0.0000	0.0000	0.0000	0.0000	0.0000	0.0164
Co1_2	0.0000	0.0000	0.0244	0.0000	0.0000	0.0000	0.0000	0.0000	0.0164
Tl1	0.0000	0.0000	0.0000	-0.0186	0.0000	0.0000	0.0000	0.0000	-0.0611
Cl1	0.0000	0.0000	-0.0481	0.0047	0.0000	0.0000	0.0000	0.0000	0.0149
Cl1_2	0.0000	0.0000	0.0240	0.0093	0.0232	0.0000	0.0000	0.0000	0.0149

Table 10: Mode decomposition of the P63 phases of different ABX3 compounds compared with mode decomposition of the P63cm phase of KNiCl3. The third column indicates the direction of the irrep distortion in the irrep space. For each compound the first column shows the amplitude of each irrep distortion, while the second indicates the value of the scalar product of its polarization vector with that of the corresponding distortion in KNiCl3, if existing. For irrep distortions only present in the P63 configuration, only thei amplitudes are indicated. The structural models have been taken from REF 48 for KNiCl3 and REF 62 for the rest.

							wR = 0.10		wR =0.15		wR =0.16	
K-vector	Irrep	dir.	Isotropys subgr.	Dim	KNiCl3		KTiCl3		KTiI3		KTiBr3	
(0,0,0)	GM2-	(a)	P6_3mc (186)	3	0.21	1	0.10	-0.9992	0.81	0.65	1.21	-0.63
(1/3,1/3,0)	K1	(a,0)	P6_3/mcm (193)	3	0.07	1	0.18	0.97	0.54	-0.91	1.09	0.90
(1/3,1/3,0)	**K3**	**(a,0)**	**P6_3cm (185)**	**2**	**1.70**	**1**	**2.11**	**-1**	**2.53**	**0.9999**	**3.73**	**0.9997**
(0,0,0)	**GM2+**	**(a)**	**P6_3/m (176)**	**1**	**0**		**0.74**		**2.04**		**1.49**	
(1/3,1/3,0)	K2	(a,0)	P6_322 (182)	1	0		0.01		0.02		0.18	
(1/3,1/3,0)	K4	(a,0)	P6_3/m (176)	4	0		0.11		0.76		2.10	

Table 11. Summary of the decomposition in symmetry-adapted distortion modes with respect to its Pm-3m parent structure of the Pnma structure of SrZrO3 (…K , REF29), NaTaO3 (REF …), and LaMnO3 (300K ,REF 64) .

Irrep	Isotropy Subgroup	Dimension	Amplitude (Å)
R4+	Imma (74)	1	1.1851
R5+	Imma (74)	2	0.0693
X5+	Cmcm (63)	2	0.3379

M2+	P4/mbm (127)	1	0.0070
M3+	P4/mbm (127)	1	0.7938

To be done …….(add wave vectors) (REDONDEAR A DOS CIFRAS DECIMALES)

Combine with the results for NaTaO3:

Summary of Amplitudes

Irrep	Isotropy Subgroup	Dimension	Amplitude (Å)
R4+	Imma (74)	1	0.9718
R5+	Imma (74)	2	0.0258
X5+	Cmcm (63)	2	0.2295
M2+	P4/mbm (127)	1	0.0133
M3+	P4/mbm (127)	1	0.7806

and For LaMnO3:

K-vector	Irrep	Direction	Isotropy Subgroup	Dimension	Amplitude (Å)
(1/2,1/2,1/2)	R4+	(a,a,0)	Imma (74)	1	1.1945
(1/2,1/2,1/2)	R5+	(-a,a,0)	Imma (74)	2	0.0890
(0,1/2,0)	X5+	(0,a,0,0,0,0)	Cmcm (63)	2	0.5649
(1/2,1/2,0)	M2+	(0,0,a)	P4/mbm (127)	1	0.3595
(1/2,1/2,0)	M3+	(0,0,a)	P4/mbm (127)	1	0.9044

Table 12. Polarization vectors of the five different irrep distortions present in the Pnma structure of SrZrO3 at K. The table shows an asymmetric unit of the Pnam structure with the positions corresponding to the parent structure. Then, the atomic displacements (in relative units) for the polarization vectors

(normalized to 1 A) of the different distortion modes are listed for the same asymmetric unit, together with their global amplitudes. Atomic displacements are expressed in relative units with respect to the corresponding supercell of the reported parent phase (a=……,c ….....) [REF29].

Reference structure:

062

5.870966 8.302800 5.870966 90.000000 90.000000 90.000000

4

Zr	1	4a	0.000000	0.000000	0.000000
Sr	2	4c	0.500000	0.250000	0.000000
O	3	8d	0.250000	0.000000	0.750000
O	3_2	4c	0.500000	0.750000	0.500000

Mode R4+:

Atom	δx	δy	δz
Zr1	0.0000	0.0000	0.0000
Sr2	0.0000	0.0000	0.0000
O3	0.0000	-0.0301	0.0000
O3_2	0.0000	0.0000	-0.0602

Mode R5+:

Atom	δx	δy	δz
Zr1	0.0000	0.0000	0.0000
Sr2	0.0000	0.0000	0.0851
O3	0.0000	0.0009	-0.0000
O3_2	0.0000	0.0000	-0.0019

Mode X5+:

Atom	δx	δy	δz
Zr1	0.0000	0.0000	0.0000
Sr2	0.0725	-0.0000	-0.0000
O3	0.0000	0.0000	0.0000
O3_2	0.0447	-0.0000	-0.0000

Mode M2+:

Atom	δx	δy	δz
Zr1	0.0000	0.0000	0.0000
Sr2	0.0000	0.0000	0.0000
O3	-0.0426	0.0000	0.0426
O3_2	0.0000	0.0000	0.0000

Mode M3+:

Atom	δx	δy	δz
Zr1	0.0000	0.0000	0.0000
Sr2	0.0000	0.0000	0.0000
O3	-0.0426	0.0000	-0.0426
O3_2	0.0000	0.0000	0.0000

Table 13: Summary of the mode decomposition of the Cmcm and P4/mbm of NaTaO3

Phase Cmcm NaTaO3 (REDONDEAR VALORES)

R4+	I4/mcm (140)	1	0.4859
R5+	I4/mmm (139)	2	0.0419

X5+ Pmma (51) 2 0.1229

M3+ P4/mbm (127) 1 0.5404

Phase P4/mbm NaTaO3

M3+ P4/mbm (127) 1 0.3790

Table 14 NbS3

K-vector	Irrep	Direction	Isotropy Subgroup	Dimension	Amplitude (Å)
(0,0,0)	GM1+	(a)	P2_1/m (11)	8	0.00
(0,0,0)	GM2+	(a)	P-1 (2)	4	0.04
(0,1/2,0)	Z1	(0,a)	P-1 (2)	12	0.52

Table 15: K2SeO4

K-vector	Irrep	Direction	Isotropy Subgroup	Dimension	Amplitude (_)
(0,0,0)	GM1+	(a)	Pnma (62)	13	0.12
(0,0,0)	GM4-	(a)	Pna2_1 (33)	8	0.55
(1/3,0,0)	SM2	(a,0)	Pna2_1 (33)	16	1.16
(1/3,0,0)	SM3	(a,0)	Pnma (62)	26	0.39

Table 16: Summary of the mode decomposition of the ninefold phase of

thiourea according to the structure reported as model 1 in REF 71 (hydrogen atoms not included).

K-vector	Irrep	Direction	Isotropy Subgroup	Dimension	Amplitude (_)
(0,0,0)	GM1+	(a)	Pnma (62)	7	0.08(1)
(0,1/9,0)	DT4	(a,-5.671a)	Pnma (62)	12	1.89(1)
(0,2/9,0)	DT1	(a,0.364a)	Pnma (62)	12	0.13(1)
(0,1/3,0)	DT4	(a,-1.732a)	Pnma (62)	12	0.19(2)
(0,4/9,0)	DT1	(a,0.839a)	Pnma (62)	12	0.09(2)

Table 17: Polarization vector of the (0,1/9,0) DT4 distortion in the ninefold phase of thiourea according to the structure reported as model 1 in REF 71 (hydrogen atoms not included).

Atom	δx	δy	δz
S1	-0.0034	0.0000	-0.0012
S1_2	-0.0098	0.0000	-0.0035
S1_3	-0.0150	0.0000	-0.0054
S1_4	-0.0196	0.0000	-0.0070
S1_5	0.0184	0.0000	0.0066
C1	-0.0012	0.0001	-0.0026
C1_2	-0.0035	-0.0001	-0.0075
C1_3	-0.0054	0.0001	-0.0114
C1_4	-0.0071	0.0000	-0.0149
C1_5	0.0066	0.0000	0.0140
N1	-0.0005	0.0002	-0.0047
N1_2	-0.0010	-0.0002	-0.0107
N1_3	0.0000	0.0002	0.0020
N1_4	-0.0013	0.0001	-0.0155
N1_5	-0.0015	0.0000	-0.0191

N1_6	-0.0010	-0.0001	-0.0138
N1_7	0.0015	-0.0001	0.0184
N1_8	0.0013	0.0001	0.0175
N1_9	0.0005	0.0002	0.0084

Table 18: Summary of the mode decomposition of the ninefold phase of thiourea according to the structure reported as model 2 in REF 71 (hydrogen atoms not included)

K-vector	Irrep	Direction	Isotropy Subgroup	Dimension	Amplitude (_)
(0,0,0)	GM1+	(a)	Pnma (62)	7	0.07(1)
(0,1/9,0)	DT4	(a,5.671a)	Pnma (62)	12	1.89(1)
(0,2/9,0)	DT1	(a,-0.364a)	Pnma (62)	12	0.14(1)
(0,1/3,0)	DT4	(a,1.732a)	Pnma (62)	12	0.16(2)
(0,4/9,0)	DT1	(a,-0.839a)	Pnma (62)	12	0.10(2)

Table 19: GaII

Order Harm.	K-vector	Irrep	Direction	Isotropy Subgroup	Dimension	Amplitude (Å)
23	(0,0,1/13)	LD3	(a,0.690a)	C222_1 (20)	2	0.11
3	**(0,0,1/13)**	**LD4**	**(a,0.690a)**	**C222_1 (20)**	**2**	**2.14**
6	(0,0,2/13)	LD1	(a,2.637a)	F222 (22)	1	0.03
20	(0,0,2/13)	LD2	(a,2.637a)	Fddd (70)	1	0.03
17	(0,0,3/13)	LD3	(a,-4.057a)	C222_1 (20)	2	0.06
9	(0,0,3/13)	LD4	(a,-4.057a)	C222_1 (20)	2	0.05
12	(0,0,4/13)	LD1	(a,-0.886a)	Fddd (70)	1	0.00
14	(0,0,4/13)	LD2	(a,-0.886a)	F222 (22)	1	0.03
11	(0,0,5/13)	LD3	(a,-0.121a)	C222_1 (20)	2	0.05

15	(0,0,5/13)	LD4	(a,-0.121a)	C222_1 (20)	2	0.11
18	(0,0,6/13)	LD1	(a,0.525a)	F222 (22)	1	0.06
8	(0,0,6/13)	LD2	(a,0.525a)	Fddd (70)	1	0.01
5	(0,0,7/13)	LD3	(a,1.905a)	C222_1 (20)	2	0.16
21	(0,0,7/13)	LD4	(a,1.905a)	C222_1 (20)	2	0.11
24	(0,0,8/13)	LD1	(a,-8.236a)	Fddd (70)	1	0.03
2	**(0,0,8/13)**	**LD2**	**(a,-8.236a)**	**F222 (22)**	**1**	**0.53**
1	**(0,0,9/13)**	**LD3**	**(a,-1.129a)**	**C222_1 (20)**	**2**	**3.59**
25	(0,0,9/13)	LD4	(a,-1.129a)	C222_1 (20)	2	0.05
22	(0,0,10/13)	LD1	(a,-0.246a)	F222 (22)	1	0.02
4	(0,0,10/13)	LD2	(a,-0.246a)	Fddd (70)	1	0.00
7	(0,0,11/13)	LD3	(a,0.379a)	C222_1 (20)	2	0.12
19	(0,0,11/13)	LD4	(a,0.379a)	C222_1 (20)	2	0.05
16	(0,0,12/13)	LD1	(a,1.449a)	Fddd (70)	1	0.04
10	(0,0,12/13)	LD2	(a,1.449a)	F222 (22)	1	0.01
13	(0,0,1)	Z2	(a,a)	C222_1 (20)	2	0.07

Figure 1

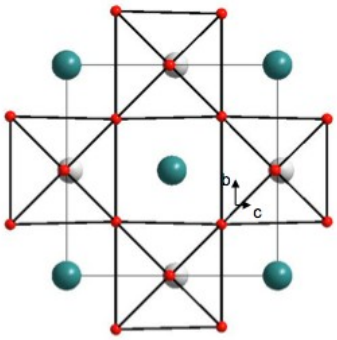

Illustration 1: Projection along the x axis of the Amm2 structure of BaTiO3 at 190K, according to [REF17].

Figure 2

Illustration 2: Scheme of the polarization vectors (projected on the plane yz) of the distortions GM4- (a) and GM5- (b) present in the Amm2 structure of BaTiO3. The figure shows in each case the distorted structure for an exaggerated amplitude of the mode. Also schematic arrows indicating the atomic displacements are depicted within a single unit cell.

Figure 3

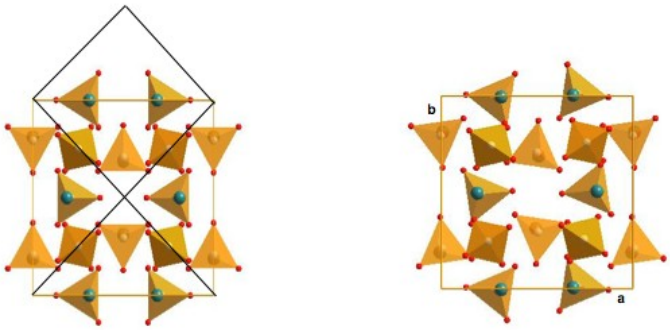

(a) (b)

Illustration 3: Structure of Gd2(MoO4)2 projected on the xy plane in the parent P-421m phase (a),and in the distorted Pba2 phase (b). The smaller tetragonal unit cell of the parent phase is indicated in (a).

Figure 4

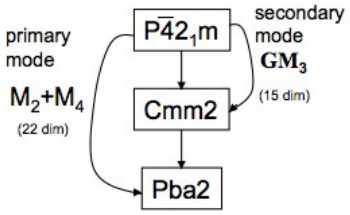

Illustration 4: Graph of maximal subgroups relating the space groups of the parent and distorted phases of Gd2(MoO4). For each subgroup, any irrep distortion compatible with it is indicated, together with the dimension of the corresponding distortion subspaces.

Figure 5

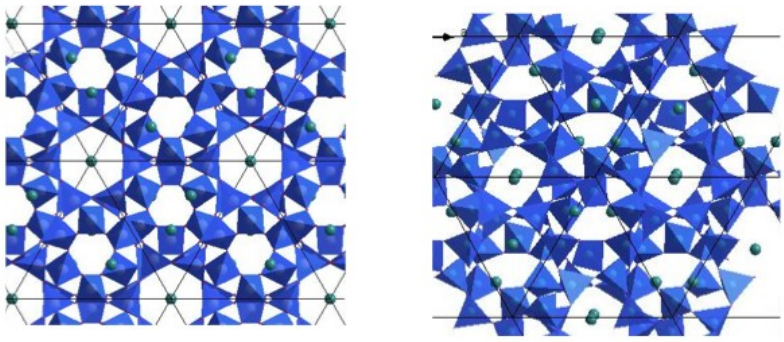

(a) (b)

Illustration 5: Structure of leucite (KAlSi2O6) projected along one of its trigonal axis in its cubic phase. (a) High temperature Ia-3d phase. (b) room-temperature tetragonal I41/a phase (REF 27)

Figure 6

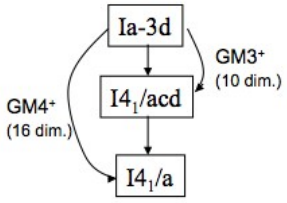

Illustration 6: Graph of maximal subgroups relating the space groups of the parent and distorted phases of leucite. For each subgroup, the irrep distortion yielding this symmetry is indicated, together with the dimension of the corresponding distortion subspace.

Figure 7

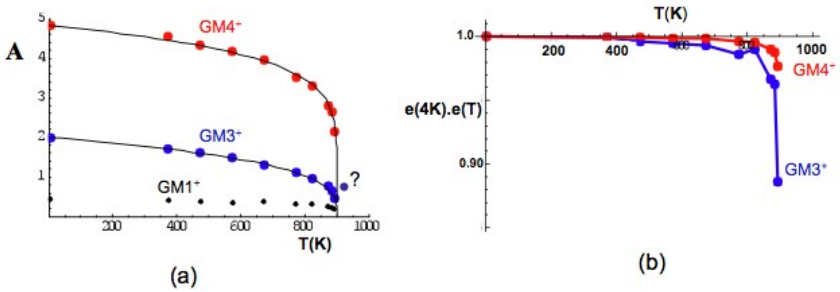

Illustration 7: (a) Temperature dependence of the amplitudes of the primary (GM4+) and secondary (GM3+) distortions in leucite, according to the structures reported in REF 27. (b) scalar product of the 16- and 10-dimensional normalized polarization vectors of the two distortions at each temperature with the corresponding one in the reported structure at 4K.

Figure 8

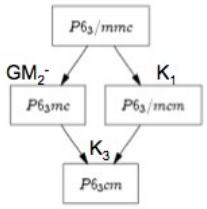

Illustration 8: Graph of maximal subgroups relating the space groups of the parent and distorted phases of KNiCl3. For each subgroup, any irrep distortion yielding this symmetry is indicated.

Figure 9 (a)

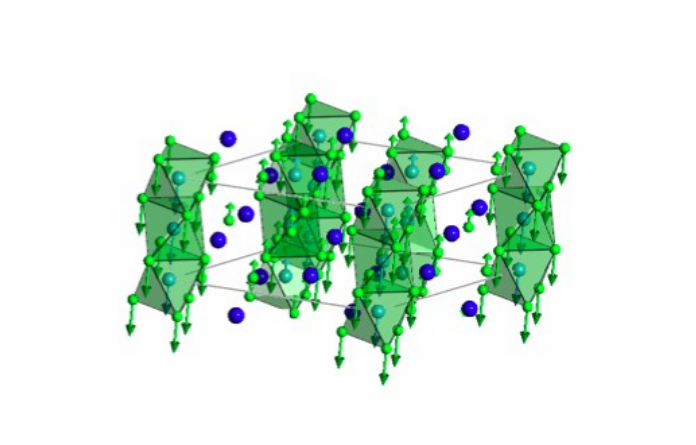

Illustration 9: Polarization vector of the distortions corresponding to the irreps K3 (a) and GM2- (b) in KNiCl3. The scale of the displacement vectors has been enlarged. (Figure has been done using FullProf Studio (REF ....))

Figure 9 (b)

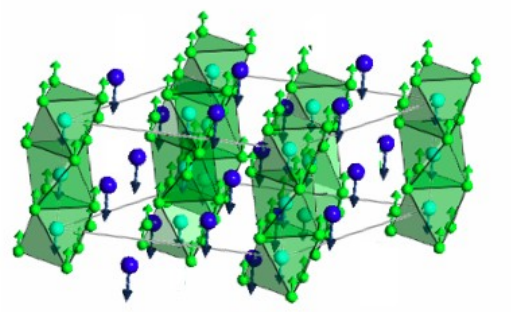

Polarization vector of the distortions corresponding to the irreps K3 (a) and GM2- (b) in KNiCl3. The scale of the displacement vectors has been enlarged. (Figure has been done using FullProf Studio (REF ....))

Figure 10

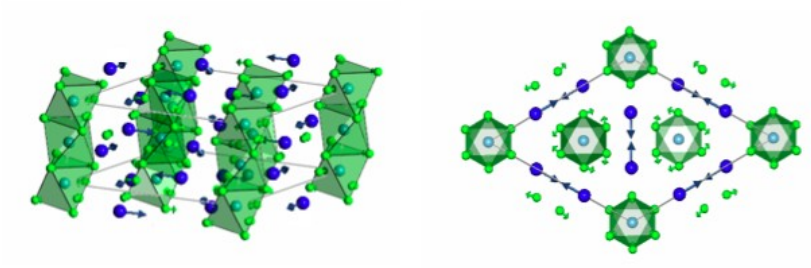

Illustration 10: Polarization vector of the distortion corresponding to the irrep K1 in KNiCl3, in a perpective view (a) and projected on the plane xy (b). The scale of the displacement vectors has been enlarged. (Figure has been done using FullProf Studio (REF …))

Figure 11

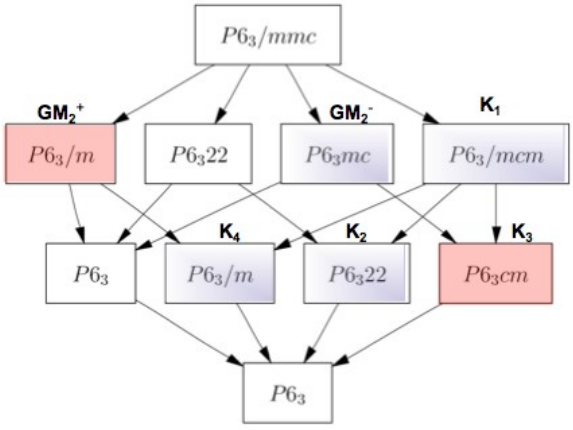

Illustration 11: Graph of maximal subgroups relating the space groups of the parent and distorted P63 phase of KTiCl3. For each subgroup, any irrep distortion yielding this symmetry is indicated. The two primary distortions evidenced by the mode decomposition of the experimental structure are highlighted.

Figure 12

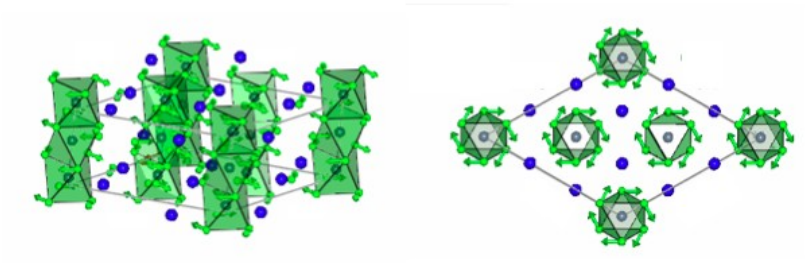

Illustration 12: Polarization vector of the primary distortion GM2+ present in the P63 structures of KTiCl3, KTiBr3 and KTiI3. (a) perspective view, (b) projection on the plane xy. The scale of the displacement vectors has been enlarged. (Figure has been done using FullProf Studio (REF …))

Figure 13

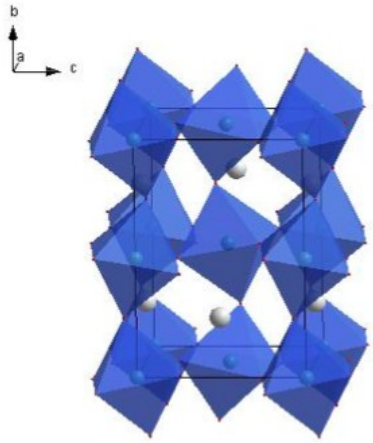

Illustration 13: scheme of Pnma SrZrO3 structure

Figure 14

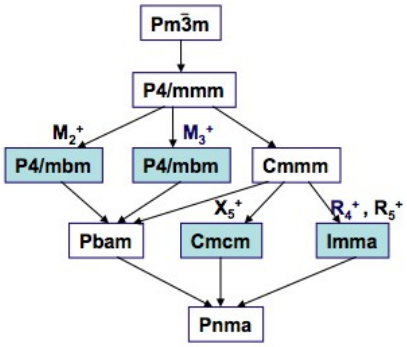

Illustration 14: Subgroup graph of SrZrO3

Figure 15

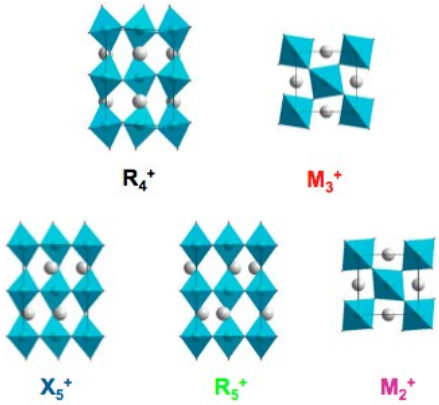

Illustration 15: Scheme of the five different irrep distortions present in SrZrO3

References:

1. general refs. on pseudosymmetric and distorted structures as high symm structure plus distortion (Hatch&Stokes, Barninghausen?, etc..)

2. books and general reviews on structural phase transitions

3. books and general references on ferroics

4. general references on Landau Theory

5. symmetry mode analyses in the literature: ours (RbCrCl3,KSeO, KniCl4, BCCD, elpasolitas, etc…), Mois, Rae, Withers, Chapon, Rabe, Ihringer, Sikora, Stokes-Utah, Karen, Bismayer, …

- Maichle, J. K., Ihringer, J. & Prandl, W. (1988). J. Appl. Cryst. 21, 22

5bis.

Author(s): PEREZ-MATO, JM; GAZTELUA, F; MADARIAGA, G; TELLO, MJ
Title: SYMMETRY-MODE ANALYSIS OF THE FERROELECTRIC PHASE IN K2SEO4
Source: JOURNAL OF PHYSICS C-SOLID STATE PHYSICS, 19 (12): 1923-1935 APR 30 1986

Author(s): MAÑES, JL; TELLO, MJ; PEREZ-MATO, JM
Title: SYMMETRY MODES AND DESCRIPTION OF DISTORTED PHASES IN HEXAGONAL ABX3 COMPOUNDS - APPLICATION TO KNICL3 ROOM-TEMPERATURE STRUCTURE
Source: PHYSICAL REVIEW B, 26 (1): 250-268 1982

Author(s): PEREZ-MATO, JM; MAÑES, JL; TELLO, MJ
Title: DYNAMICAL ASPECTS AND THERMODYNAMIC THEORY OF THE ALPHA-BETA-PHASE TRANSITION IN RBCRCL3 AND CSCRCL3 CRYSTALS
Source: JOURNAL OF PHYSICS C-SOLID STATE PHYSICS, 13 (14): 2667-2674 1980

Author(s): Aroyo, MI; Perez-Mato, JM
Title: Symmetry-mode analysis of displacive phase transitions using International Tables for Crystallography
Source: ACTA CRYSTALLOGRAPHICA SECTION A, 54: 19-30 Part 1 JAN 1 1998

Author(s): EZPELETA, JM; ZUNIGA, FJ; PEREZ-MATO, JM; PACIOREK, WA; BRECZEWSKI, T
Title: STRUCTURAL-ANALYSIS OF THE FOURFOLD PHASE OF BETAINE CALCIUM-CHLORIDE DIHYDRATE AT 90-K

Source: ACTA CRYSTALLOGRAPHICA SECTION B-STRUCTURAL SCIENCE, 48: 261-269 Part 3 JUN 1 1992

6. Programs: Isodisplace, Kirova, Wills, symmodes, Basireps Juan

Ritter, H., Ihringer, J., Maichle, J. K. & Prandl,W. (1998). SIMREF26, http://www.uni-tuebingen.de/uni/pki/simref/simref.html.

7. Refs. Al Bilbao server

8. ref. Amplimodes: to be published …

9. FullProf

10. Campbell: Newsletter WO3

12 Wyckoff splitting (Wondratschek …)

13. definition of isotropy group (Hatch&Stokes)

14. term secondary modes in symmetry sense [Ascher?, Hatch & Stokes ???]

15. general refs. ferroelectrics (Lines&Glas, K. Rabe book)

16. general references on phase diagram of BaTiO3

17. ref. on range of phase Amm2 of BaTiO3: Tomazewski article

18. Amm2 structure BaTiO3 Kwei et al. (1993)

19. Notation of irreps: Hatch&Stokes isotropy

20. reference for notation T1u etc…

21-bis. Faintness index

22. Von Neumann principle

23- general reference: improper ferroelectric

24 referencias sobre Molybdato de gadolinio como ferroelectrcio impropio (Dvorak)

25 Jeitschko (1972)

26 reference for physically irreducible

26-bis referencia on equivalent descriptions of a structure through the use of normalizer or specialized normalizer

27. DAVID C. PALMER,!'* MARTIN T. DOVE,! RICHARD M. IBBERSON,2 ANDBRIAN M. POWELL3. Amer. Miner. 82 (1997) 16

28. Lange, R.A., Carmichael, LS.E., and Stebbins, IF. (1986) Phase transitions in leucite KAISi206, orthorhombic KAISiO" and their iron analogues (KFeSi,06' KFeSiO,). American Mineralogist, 71, 937-945.

29 –references RUMs:

K.D. Hammonds, M.T. Dove, A.P. Giddy and V. Heine, Am. Miner. 79 (1994) 1207-1209.

M.T. Dove, A.K.A. Pryde, V. Heine and K.D.Hammonds, J.Phys.:Cond.Matt. 19 (2007) 275209:1-20.
M.T. Dove, A.K.A. Pryde and D.A. Keen, Miner. Mag. 64(2) (2000) 267-283.

referencias_generales perovskitas:
30 . Acta Cryst. (1972). B28, 3384-3392
[doi:10.1107/S0567740872007976]
The classification of tilted octahedra in perovskites
i) M. Glazer

31 Woodward, P. M. (1997). Acta Cryst. B53, 32±43.
32 Woodward, P. M. (1997). Acta Cryst. B53, 44±66.

32 bis Avdeev M. Caspi E.N., Yakovlev S., Acta Cryst. B 63 (2007) 363

33 Group-Theoretical Analysis of Octahedral Tilting in Perovskites
Christopher J. Howard and Harold T. Stokes
Acta Cryst. (1998). B54, 782±789

34- Normal-mode analysis of the structures of perovskites with tilted octahedra

C. N. W. Darlington, Acta Cryst. (2002). A58, 299±300

35- Title: The structural phase transitions in strontium zirconate revisited

Author(s): Howard CJ, Knight KS, Kennedy BJ, et al.

Source: JOURNAL OF PHYSICS-CONDENSED MATTER Volume: 12 Issue: 45 Pages: L677-L683 Published: NOV 13 2000

36- Title: High-temperature phase transitions in SrZrO3

Author(s): Kennedy BJ, Howard CJ, Chakoumakos BC

Source: PHYSICAL REVIEW B Volume: 59 Issue: 6 Pages: 4023-4027 Published: FEB 1 1999

37 Phys. Rev. Lett. 74, 2587 - 2590 (1995)

Competing Structural Instabilities in Cubic Perovskites

W. Zhong and David Vanderbilt

38- General reference of hatch & Stokes on isotropy subgroups, “directions” for the order parameters, etc… (probably already cited in the first references to decide above)

39 Monoclinic and triclinic phases in higher-order Devonshire theory

David Vanderbilt and Morrel H. Cohen

Phys. Rev. B 63, 094108 (2001)

40 Fu, W.T., Ijdo, D.J.W., J. Solid State Chem. 179, 2732

41.

Powder neutron diffraction study of the high temperature phase transitions in Na Ta O3.

Authors Kennedy, B.J.;Prodjosantoso, A.K.;Howard, C.J.

Reference Journal of Physics: Condensed Matter (1999) 11, 6319-6327

42 janssen, Tablas Internacionales, chapter on superspace ….

43

Author(s): Perez-Mato, JM

Title: Superspace description of commensurately modulated structures

Source: Methods of Structural Analysis of Modulated Structures and Quasicrystals, Eds. Perez-Mato, JM; Madariaga, G; Zúñiga, FJ: 117-128 1991

Ed: Word Scientific, Singapore 1991

44. F. Parisi, Phys Rev B. analysis de la fase lock-in del KSeO del argentino ….

45 descomposicion en modes del K2SeO4 (ya citado seguramente en una de

las citas generales iniciales)

46 referencia general perovskitas hexagonales con prototipo CsNiCl3

47 Referencia sobre KNiCl3 y familia y sus propiedades ferroelectricas

48 KNiCl3 estructura:

Visser, D.;Verschoor, G.C.;Ijdo, D.J.W. Acta Crystallographica B (1980) 36, 28-34

49 Mañes et al (seguramente ya indicada en las generales de la introduccion) :

PHYSICAL REVIEW B VOLUME 26, NUMBER 1 1 JULY 1982

Symmetry modes and description of distorted phases in hexagonal ABX_3 compounds. Application to $KNiCl_3$ room-temperature structure

J. L. Mañes, M. J. Tello, and J. M. Pérez-Mato
Departamento de Fisica, Facultad de Ciencias, Universidad del Pais Vasco, Apdo 644, Bilbao, Spain
(Received 26 January 1982)

50 referencias Nenert e Ihringer sobre el YMnO3 (del paper sobre AMPLIMODES)

51 paper amplimodes JAPC to be published

52 Fennie and rabe, YMnO3

53 Japoneses sobre ferrielectricidad en el KNiCl3:

[1] K. Machida, T. Mitsui, T. Kato, and K. Iio, Solid State Commun. **91**, 17 (1994).

54 Domains- chapter from International Tables?

55: Structure de Tl Fe Br3: Distorsion du type perovskite hexagonale 2L.

Authors Jouini, N.;Guen, L.;Tournoux, M.

Reference Materials Research Bulletin (1982) 17, 1421-1427

56: Die Kristallstruktur des Raumtemperatur-Rubidium-Tribromomanganats(II).

Authors Fink, H.;Seifert, H.J.

: Acta Crystallographica B (1982) 38, 912-914

57. Crystal and magnetic structures of 2H Ba Mn O3.

Authors Cussen, E.J.;Battle, P.D.

Reference Chemistry of Materials (2000) 12, 831-838

58: Neutron diffraction study of distorted-triangular-lattice Ising-like antiferromagnet Tl Co Cl3.

Authors Nishiwaki, Y.;Kato, T.;Oohara, Y.;Oosawa, A.;Todoroki, N.;Igawa, N.;Ishii, Y.;Iio, K.

Reference Journal of the Physical Society of Japan (2006) 75, 034707-1-034707-8

59: Inorganic crystal structure database

60: Neutron Powder Diffraction and Magnetic Measurements on Rb Ti I3, Rb V I3, and Cs V I3.

Authors Zandbergen, H.W.

Reference Journal of Solid State Chemistry (1981) 37, 308-317

61: Rae et al. Aurivillius SBT (probablemente ya citado en la introduccion)

62: Divalent Titanium: The Halides ATiX3 (A _ K, Rb, Cs; X _ Cl, Br, I)

Liesbet Jongen, Thomas Gloger, Jan Beekhuizen, and Gerd Meyer

Z. Anorg. Allg. Chem. **2005**, *631*, 582_586

63. dos Papers de Howard en el ultimo Acta Cryst, sobre Jahn-Teller en perovskitas

64. J. Rodrıguez-Carvajal, M. Hennion, F. Moussa, and A. H. Moudden L. Pinsard and A. Revcolevschi, Phys Rev B 57 (1998) R3189

65. S. van Smaalen, Phys. Rev B 38 (1988) 9594

66. J. Rijnsdorp and F. Jellinek, J. Solid State Chem. 25, 325 (1978)

67 Ref. JANA

68.

Author(s): Aramburu, I; Friese, K; Perez-Mato, JM; Morgenroth, W; Aroyo, M; Breczewski, T; Madariaga, G
Title: Modulated structure of Rb2ZnCl4 in the soliton regime close to the lock-in phase transition
Source: PHYSICAL REVIEW B, 73 (1): Art. No. 014112 JAN 2006
ISSN: 1098-0121

69 MOUDDEN, A. H., DENOYER, F., LAMBERT, M. St. FITZGERALD, W.

(1979). *Solid State Commun.* 32, 933-936.

70

Author(s): ZUNIGA, FJ; MADARIAGA, G; PACIOREK, WA; PEREZ-MATO, JM; EZPELETA, JM; ETXEBARRIA, I

Title: MODULATED STRUCTURE OF THIOUREA

Source: ACTA CRYSTALLOGRAPHICA SECTION B-STRUCTURAL SCIENCE, 45: 566-576 Part 6 DEC 1 1989

71

S. Tanisaki, H. Mashiyama, K. Hasebe, Acta Cryst. B44 (1988) 441-445

72

Author(s): PEREZ-MATO, JM; MADARIAGA, G; TELLO, MJ

Title: IRREDUCIBLE REPRESENTATIONS OF SPACE-GROUPS AND SUPERSPACE SYMMETRY

Source: FERROELECTRICS, 53 (1-4): 293-296 1984

73

Author(s):; Perez-Mato, JM; Elcoro, L; Aroyo, MI.; Katzke, H; Toledano, P; Izaola, Z
Title: Apparently complex high-pressure phase of gallium as a simple modulated structure
Source: PHYSICAL REVIEW LETTERS, 97: 115501 SEP 2006
ISSN: 0108-7681

74

Structural Complexity in Gallium under High Pressure: Relation to Alkali Elements
O. Degtyareva,* M. I. McMahon, D. R. Allan, and R. J. Nelmes

Phys. Rev. Lett. 93, 205502 (2004) [4 pages]